Universidade de Aveiro
2017

Departamento de Engenharia de Materiais e Cerâmica

Gonçalo da Costa Ramalho

Development and optimization of biomimetic PCL electrospun scaffolds for cartilage tissue engineering

Desenvolvimento e optimização de estruturas porosas de PCL por electrofiação para engenharia de tecidos da cartilagem

Universidade de Aveiro
2017

Departamento de Engenharia de Materiais e Cerâmica

Gonçalo da Costa Ramalho

Development and optimization of biomimetic PCL electrospun scaffolds for cartilage tissue engineering

Dissertação apresentada à Universidade de Aveiro para cumprimento dos requisitos necessários à obtenção do grau de Mestre em Materiais e Dispositivos Biomédicos, realizada sob a orientação científica do Doutor António Manuel Godinho Completo, Professor Auxiliar com Agregação do Departamento de Engenharia de Mecânica da Universidade de Aveiro e da Doutora Paula Alexandrina de Aguiar Pereira Marques, equiparada a Investigadora Principal no Departamento de Engenharia Mecânica da Universidade de Aveiro.

O júri

Presidente

Profª. Doutora Isabel Margarida Miranda Salvado

Professora Associada, Universidade de Aveiro

Prof. Doutor Rui Ramos Ferreira e Silva

Professor Associado, Universidade de Aveiro

Doutora Paula Alexandrina de Aguiar Pereira Marques

Equiparada a Investigadora Principal, Universidade de Aveiro

Relembra o passado e aprende com ele. Sonha com o futuro. Mas vive no presente.

Agradecimentos

Primeiramente, e desta forma mais formal, gostaria de agradecer à minha família, aos meus pais e irmãos, pelos sacrifícios feitos porque sem eles nada disto seria possível (todo o meu percurso académico e de enriquecimento pessoal e cultural). Agradeço a sua constante presença, amizade, amor, e pela força e deposição de confiança que dão nas escolhas que eu tomo para a minha vida. Um grande obrigado por serem quem são, não vos trocaria por nada deste mundo!

Gostava de agradecer ao professor António Completo e à professora Paula Marques pela oportunidade que me deram para fazer parte desta equipa, pelos seus conselhos e disponibilidade, e por me permitirem "fazer ciência".

Um obrigado à Universidade de Aveiro e ao DEMaC pela oportunidade e disponibilidade, quer na resolução de problemas, quer na disponibilidade de recursos.

Um grande obrigado ao meu parceiro, colega de trabalho e amigo André Girão, que se mostrou disponível desde o início para me ajudar em tudo o que fosse preciso para a resolução da dissertação. E mais que tudo, um obrigado pela amizade. Foste uma boa surpresa.

Um especial obrigado à Ângela Semitela, pela constante ajuda prestada na resolução da tese, e pela sua característica emoção e vontade em trabalhar. Uma boa amizade aqui fica.

À Susana Pinto pelos conselhos, mesmo que não interferindo directamente no meu trabalho, se mostrou sempre disponível para ajudar. E claro, a sua boa disposição e humor contagiantes.

Ao meu pessoal do GOTA, por me deixarem ser quem realmente sou e me deixarem transpirar a minha veia artística!

Ao Paulo Pinho por ser o grande amigo que é, e por todas as nossas insanas vivências. Um obrigado especial a esta amizade, que se revela cada vez mais importante.

A todos os meus amigos que estiveram presentes na minha vida. Quer pelo apoio, quer pelas risadas, quer pelas mais diversas discussões dos temas que ocupam as nossas vidas. Um especial obrigado ao meu grande amigo de infância Manuel Santos, ao Miguel Gaspar pela partilha de interesses semelhantes e pela amizade, ao Hugo Almeida porque ele sabe porquê, à Adriana Magueta pela amizade boa e saudável que temos, à Janice Rocha pelas suas maluqueiras e amizade. E a todos os outros que apenas não estão aqui incluídos porque tenho que terminar o texto, porque senão vão-me chatear por me prolongar muito.

This work was partially supported by the funding of Program COMPETE-FEDER, Programa Operacional Competitividade e Internacionalização through the project POCI-01-0145-FEDER-016574 and by Fundação para a Ciência e Tecnologia I.P. (FCT, IP) through the project PTDC/EMS-TEC/3263/2014.

Palavras-chave Cartilagem articular; Condrócitos; Engenharia de tecidos; Scaffolds nanofibrosos; Policaprolactona; Electrofiação.

Resumo

As lesões na cartilagem articular são um grande problema da sociedade actual. A engenharia de tecidos da cartilagem é uma alternativa emergente aos procedimentos da medicina tradicional, produzindo estruturas porosas biomiméticas capazes de mimetizar a organização estrutural das fibras de colagénio, dependentes de profundidade, da cartilagem articular nativa. O presente trabalho, pretendia não só optimizar o tamanho dos poros da estrutura fibrosa electrofiada das várias zonas que compõem as estruturas porosas 3D anisotrópicas, desenvolvidas anteriormente pelo grupo de investigação da equipa de supervisão, como também recombinar estas zonas electrofiadas em arquitecturas fibrosas 3D alternativas. Para atingir este objectivo, três diferentes zonas de Policaprolactona (PCL) electrofiado foram montadas em diferentes arranjos dentro do hidrogel de óxido de grafeno (GO)-colagénio de modo a serem capazes de providenciar uma malha porosa apta para protocolos de cultura de células, depois do processo de liofilização. Estas estruturas porosas de PCL-GO-colagénio foram caracterizadas de forma a avaliar a influência do tamanho e orientação das fibras nas propriedades finais da estrutura 3D. Foram feitos testes de biocompatibilidade com condrócitos em cultura estática nas diferentes zonas fibrosas que compõem a estrutura porosa. Apesar dos resultados de biocompatibilidade serem promissores, estes mostraram que existe necessidade de continuar a optimização da porosidade das zonas fibrosas de forma a promover/facilitar a migração celular através da estrutura porosa antes de se fazer ensaios de culturas celulares em ambiente dinâmico num bioreactor.

Keywords Articular Cartilage; Chondrocytes; Tissue Engineering; Nanofibrous Scaffolds; Polycaprolactone, Electrospinning.

Abstract

Injuries of the articular cartilage are a huge problem in the present society. Cartilage tissue engineering is emerging as an alternative to traditional medical procedures by producing biomimetic scaffolds capable of mimicking the depth dependent nanostructural organization of the fibrous collagen network of the native articular cartilage. This work intended not only to optimize the pore size of the fibrous electrospun zones that comprise a 3D anisotropic scaffold previously developed by the research group of the supervision team, but also to recombine these electrospun zones in alternative fibrous 3D architectures. To achieve this goal, three electrospun polycaprolactone (PCL) zones were assembled in different arrangements within a graphene oxide (GO)-collagen hydrogel capable of providing a suitable porous network for cell culture protocols after a lyophilisation process. These PCL-GO-collagen scaffolds were characterized with the purpose of evaluating the influence of the fibres size and orientation on the final properties of these 3D structures. Preliminary biocompatibility tests on the different fibrous zones that compose the scaffolds were assessed with chondrocytes static cultures. Although the biocompatibility results were promising, the outcomes showed the need of the continuous optimization of the porosity of the scaffold fibrous zones in order to promote/facilitate the cell migration through the whole scaffold before starting the dynamic cell culture in a bioreactor.

Index

Figures List

Table List

Chapter 1

INTRODUCTION

1.1. Framework

Osteoarthritis is a chronic rheumatic condition, which is a degenerative disease that mainly affects the articular cartilage. It is claimed by the World Health Organization that osteoarthritis is one of the most disabling disease in developed countries. Indeed, symptomatic osteoarthritis is estimated to affect 9.6% of men and 18.0% of women aged over 60 years, causing serious limitations in movement. This is where cartilage tissue engineering could interfere in order to produce materials capable of recreating an *in vitro* tissue capable of mimicking the depth dependent nanostructural organization of the fibrous collagen network of the native articular cartilage by combining biomaterials and cells with suitable fabrication techniques [1].

One of these biomaterials is Polycaprolactone (PCL). PCL is a semi-crystalline polymer with a hydrophobic nature; it exhibits a very slow degradation rate (2–4 years depending on the starting molecular weight) that finds many applications in biomedical science owing to its superior mechanical properties, good biocompatibility, and complete degradation to nontoxic by-products. It is also a Food and Drug Administration approved material [2].

Additionally, PCL is commonly used for the production of multilayer electrospun scaffolds by varying both the fibre size and orientation would create scaffolds with different topographic and mechanical properties [2].

In this study it was prepared four different fibrous/porous architectures of PCL–Graphene Oxide-collagen (PCL-GO-collagen) scaffolds aiming to bring together the advantages of the synthetic PCL, biocompatibility of collagen and the biochemical and mechanical properties of GO in order to mimic the anisotropic structure of the natural articular cartilage. The inclusion of collagen into PCL nanofibers was considered favourable to cell attachment [2]. Electrospinning was used as fabrication technique and the operating conditions were adjusted to obtain anisotropic scaffolds.

At the end, the different electrospun zones that compose the scaffolds, as well as the PCL-GO-collagen scaffolds were morphologically, mechanically and biologically tested.

The work developed in this thesis is integrated in the project “ARCADELIKE – DESENVOLVIMENTO DA ARQUITETURA FISIOLÓGICA DA CARTILAGEM DESENVOLVIDA IN-VITRO POR COMBINAÇÃO DE ESTÍMULO MECÂNICO E SCAFFOLDS FIBROSOS ANISOTRÓPICOS EM BIORREACTOR” (REF. PTDC/EMS-TEC/3263/2014). The main objective of this project is to develop and fabricate anisotropic fibrous PCL scaffolds with depth-dependent variations in the fibrillar size and orientation in order to see how these variables dictate physical and mechanical properties, as well as the cellular response in both static and dynamic (mechanical stimulation) cultures. Also, this work is a sequence of a previous one that achieved a 3D fibrous scaffold with distinct biomimetic zones through the assembly of electrospun PCL fibres with different orientations by varying the electrospinning conditions [3].

1.2. Objectives

This work is intended to optimize the original fabrication technique, the mechanical properties of the scaffold and its biocompatibility. Thus, briefly, the goals of this thesis are:

I) Optimization of the pores size of the electrospun PCL 3D structure in order to enhance the cell proliferation and migration towards the scaffold.

II) Fabrication and characterization of four scaffolds with different anisotropic properties with the purpose of being used as alternative enhanced cartilage *in vitro* microenvironments able to promote cartilage regeneration by using different pathways. Indeed, we expect that the distinct anisotropic signatures of each scaffold could offer similar mechanical and topographical characteristics and then, theoretically, influence the cell behaviour differently.

III) Evaluation of the biocompatibility of the different electrospun PCL zones that compose the 3D anisotropic fibrous structures.

1.3. Document Organization

This dissertation is divided into six chapters. This first chapter presents a short introduction, which includes a framework of the theme and the objectives of the dissertation. The second chapter exposes the state of the art with some concepts about

the natural articular cartilage, its constituents and tissue engineering (TE) related to it, scaffolds and nanofibrous scaffolds and the polymer polycaprolactone (PCL). The third chapter describes the methodology and the materials required to execute the experimental work. Results and their discussion are presented at chapter four. The fifth chapter presents the main conclusions taken from this work, and some suggestions for future work. Then it follows the references of the citations made in the work and finally annexes.

Chapter 2

STATE OF THE ART

This chapter introduces the main concepts that fundament the experiments described in this thesis, such as the anatomy of native articular cartilage (section 2.1) and the potential of TE techniques as alternative treatments for repairing the injured cartilaginous tissue (section 2.2) focusing on the significance of Polycaprolactone (PCL) biocompatible scaffolds (sections 2.3 and 2.4).

2.1. Articular Cartilage

Articular cartilage is a specialized connective tissue that covers the ends of synovial joints that allows the transmission of physiological loads to the underlying subchondral bone and friction-free movement of articulating joints providing the basis for the movements of an organism. Since it is avascular (no blood supply) and aneural (no nerve endings), native cartilage owns a poor capacity to heal after injury [4][5].

The articular cartilage is organized into three different zones (Figure 1) that are assembled in a depth-wise dependent hierarchical structure defined as follows: 1) a superficial zone which is composed mainly by collagen type II fibres produced by chondrocytes that are oriented parallel to the surface of the subchondral bone surface; 2) a middle zone composed by collagen fibres randomly oriented; 3) a deep zone, where the collagen fibres are oriented perpendicularly to the surface on the interface cartilage-bone [6]. Additionally, there are even who considers a fourth zone, this being the final one and called the calcified zone, which is responsible to connect the cartilage tissue to the underlying subchondral bone [7,8]. The superficial zone makes up 10% to 20% of the total cartilage volume and has the highest amount of collagen. Having the highest amount of collagen translates in high tensile modulus, making this zone resistant to shear, tensile and compressive forces imposed by the articulation at the joint surface. The middle zone has around 40% to 60% of the total cartilage volume and is mostly composed of negatively charged proteoglycans (forming the hyaline cartilage), which in turn attract

positive charges accompanied with water, making it a stable hydrated structure. The proteoglycans present in the middle zone are what gives the cartilage its compression-resistance properties due to the fact that it maintains the fluid within the tissue of the cartilage while it is being compressed. The deep zone represents 30% of articular cartilage and is responsible for providing the greatest resistance to compressive forces, since it has the collagen fibrils arranged perpendicularly to the articular surface [6,9].

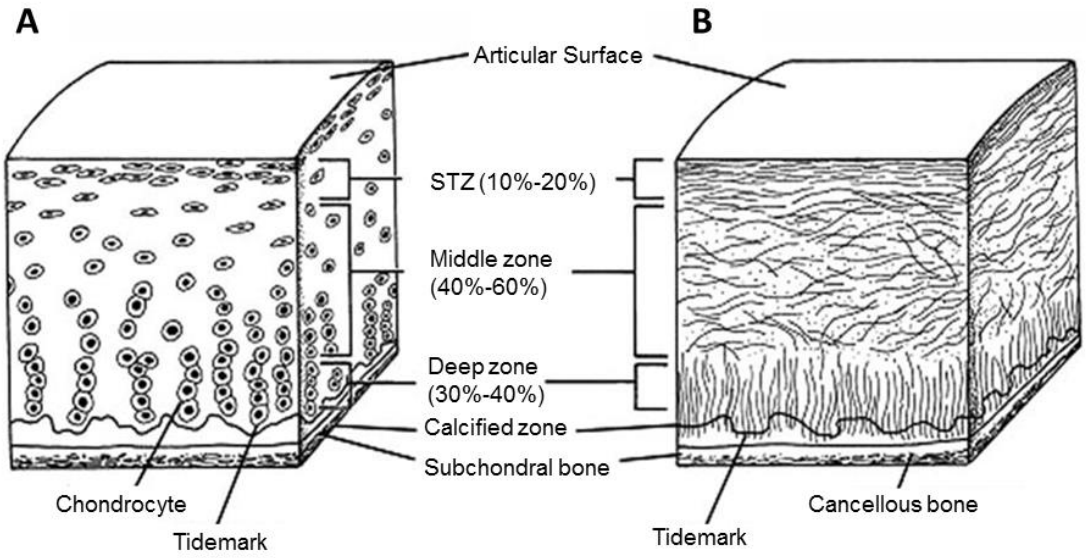

Figure 1 - Section of cartilage with the three different zones: superficial tangential zone (STZ), middle zone and deep zone. A – cellular organization in the zones of articular cartilage; B – collagen fibre architecture. Adapted from: [9]**.**

The cells that reside within the cartilage are chondrocytes, a highly specialized cell line that represents only 2% of the total tissue volume, being responsible for maintaining and producing the extra-cellular matrix (ECM), mainly collagen fibres and proteoglycans. The combination of these components with inorganic salts, small amounts of other proteins, lipids and glycoproteins is able to provide a suitable microenvironment capable of efficiently retaining water and consequently enhance the biomechanical properties, guaranteeing the functional behaviour of the cartilage [9,10]. The diffusion of nutrients and waste is possible due to the cyclical compression of the articular cartilage providing chondrocyte homeostasis and a stale ECM which in turn provides the articular cartilage frictionless joint and a stiff load-bearing tissue to absorb energy [11].

Cartilage self-repair ability is very limited since it is an avascular tissue rich in ECM, but low in cell density (because of low mitotic potential of the chondrocytes). This is why cartilage lesions caused by trauma or diseases tend to progressively degrade the tissue and also originate diseases such as osteoarthritis. Indeed, small defects are healed with the migration of chondrocytes, but the big defects are healed with fibrillar cartilage which turns out to be insufficient [4,5,10,12]

2.1.1. Chondrocytes

Chondrocytes are the resident cells of the hyaline articular cartilage. These highly specialized cells are responsible for the production of the basic ECM constituents: proteoglycans and collagen type II. Therefore they have an important role in maintenance, repair, development and remodelling of the cartilage ECM [9,12].

Chondrocytes are originated from mesenchymal stem cells and make up to 2% of total volume of articular cartilage. Also, depending on the anatomical regions of the cartilage, they vary in shape, number and size (Figure 2). In the superficial zone, chondrocytes are flatter, smaller and have greater density, enabling resistance to shear and tensile forces and, additionally, protecting and maintaining the deeper layers. In the middle zone, chondrocytes are spherical and have low density, making this zone the first line of resistance to compressive forces. While in the deep zone, chondrocytes are typically arranged in columnar orientation, parallel to the collagen fibres and perpendicular to the joint line, providing the greatest amount of resistance to compressive forces. They respond to different stimuli, such as growth factors, mechanical loads, hydrostatic pressures and piezoelectric forces. However, their potential for replication is limited, making cartilage healing a problem [9,13].

Chondrocytes are therefore essential for studies related to cartilage TE but when cultured in vitro they tend to dedifferentiate (that is, they lose their special form or function, or revert to an earlier developmental stage). So, supplemented medium and three-dimensional culture structures are used to maintain the chondrocyte phenotype [12]. Also, chondrosenescence (the deterioration of chondrocyte function related to age-dependency) contributes for the age-related deregulation of subcellular signalling pathways in chondrocytes, which in turn decreases the synthetic capacity of the cartilage leading to the manifestation of diseases such as osteoarthritis [14,15].

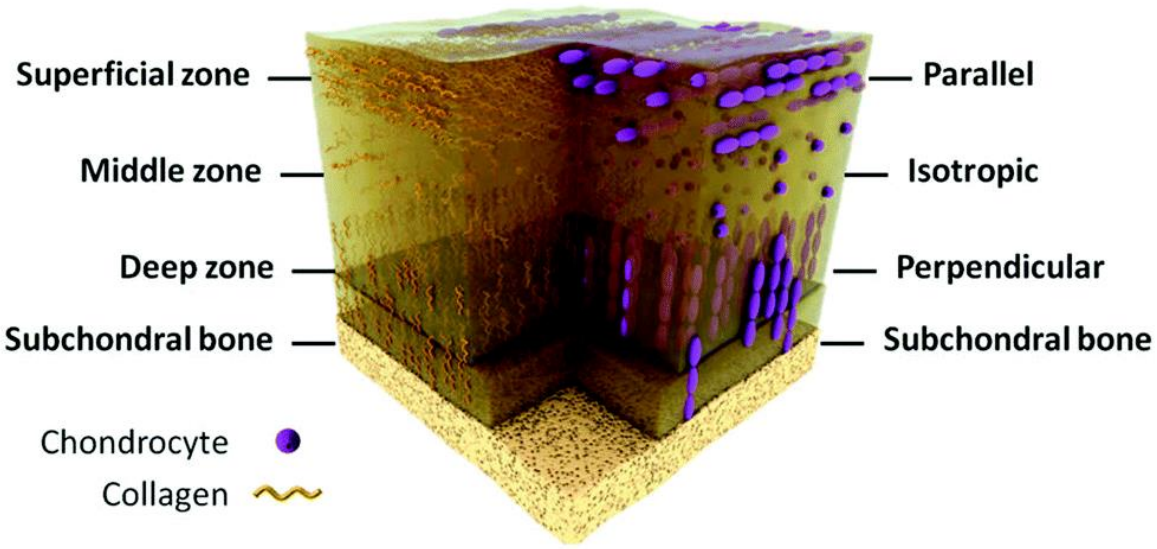

Figure 2 - Schematic representation of the multi-zonal structure of normal articular cartilage showing the collagen and cell orientation. Adapted from[16]**.**

2.1.2. Collagen and Proteoglycans

Collagen fibres (Figure 3) are one of the most common proteins in the body. It is mainly organized with three procollagen polyptide chains (approximately 100 amino acids each) that are coiled in a α-helix to make what is called tropocollagen, which in turn assembles into larger fibres that crosslink in order to provide tensile strength. It's diameter in articular cartilage is between 25-40 nm in size [10,17]. Collagen is a natural polymer found in skin, bone, blood vessels, cornea, cartilage, gut, inter-vertebral disc, tendons and ligaments and comprises approximately 25%-35% of total body protein in the form of elongated fibrils. It possesses good tensile strength and elasticity and it can be found outside and inside the body cells providing support to body tissues [18,19]. In the collagen family there are 28 genetically distinct collagen types, being the most abundant the collagen type I (skin, tendon, and bone), collagen type II (cartilage), and collagen type III (skin and vasculature). These fibrillar structures are essential for tissue architecture and integrity. [17].

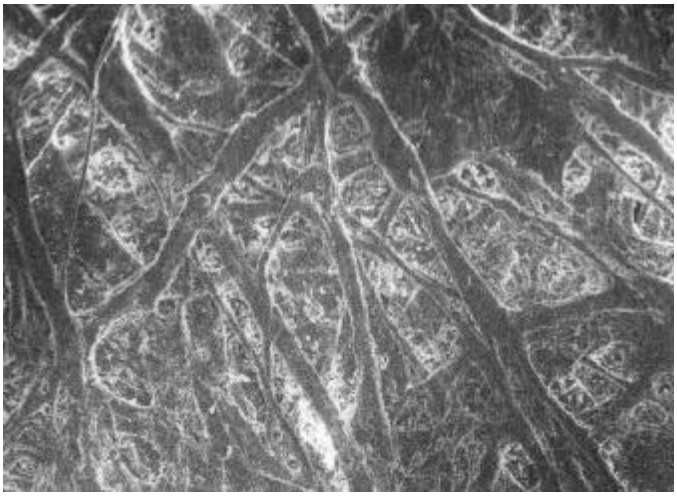

Figure 3 - Collagen fibres (with sizes that could vary between 40-100 nm in skin) from the surface of parchment, as shown by Scanning Electron Microscopy. 123x magnification. Adapted from [20]

Proteoglycans are made of polysaccharide-protein compounds with a ratio of 95% polysaccharide and 5% of protein, and can exist in monomer or aggregates. In the core we can find the polar polysaccharide glycosaminoglycan (GAG) which is covalently linked to the proteoglycans, acting as lubricant and shock absorber. It is also responsible for maintaining osmotic pressure which is essential to keep the equilibrium between the external stress caused and the fluid flow in the ECM, complementing the tensile strength of the collagen fibres [10,21]. Proteoglycans influence nucleation and growth in developing fibres and fibre diameter in mature fibres. They are anionic in nature and they can bind with collagen (Figure 4) through non-covalently bindings [20].

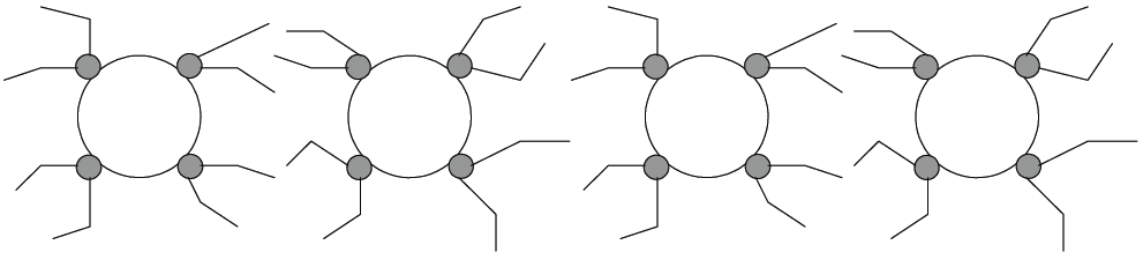

Figure 4 - Diagrammatic representation of the binding of proteoglycan groups to collagen fibrils. The four big white circles represent the collagen fibrils, viewed down the main fibril axis. The shaded circles represent the protein core of the proteoglycans. The lines emanating from the protein cores are representative of the branched glycosaminoglycan (GAG) chains of the proteoglycans. Adapted from [20]**.**

2.2. Cartilage Tissue Engineering

Cartilage TE emerges from a growing need to create a more durable and functional replacement for the degenerated tissue of the native cartilage. The solution must be able to resist and operate in the same biochemical and mechanical conditions that the natural cartilaginous tissue is submitted to. The current clinical treatments, such as mosaicplasty, autologous chondrocytes injection, osteochondral autograft transplantation, osteochondral allograft transplantation and microfracture, show unsatisfactory long-term results, because of the new tissue formed lacking structural organization and having inferior mechanical properties when compared to the native tissue. Furthermore, cultured chondrocytes, both *in vitro* or *in vivo*, tend to dedifferentiate into fibroblast-like shape, changing the production from collagen type II into type I (typical for fibrillar cartilage and mature bone, which has a fibrous network) and consequently affecting the functional features of the cartilaginous tissue [12,22].

Usually, damage to the articular cartilage can be due to congenital anomalies, degenerative joint diseases (such as osteoarthritis) and traumatic injuries, which can affect every group age and are very painful. Since natural cartilage has an insufficient self-repair mechanism due to its avascular and aneural nature, low level of chondrocytes density, low proliferative activity and the tendency of chondrocytes to de-differentiate, treatment of damaged articular cartilage constitutes a challenge [12,23]. In fact, it is affirmed by Kock *et al.* [24] that osteoarthritis could affect all ages and around 70% of people aged >65 years is affected by this disease. Also, Klein *et al.* [1] claims that osteoarthritis affects around 27 million Americans, and 6.6 million people in England alone [25]. In fact, according to the World Health Organization, in 2010, among 289 diseases, osteoarthritis was considered the eleventh leading cause of years lived with disability, becoming then a research priority in the European Community countries [26]. Additionally, in the coming years the tendency to develop some type of osteoarthritis could get as high as 25% of the world population, making alternative approaches to the treatment of this disease be particularly valuable [27].

Taking all this into account, the goal and also the biggest challenge of cartilage TE is to recreate an *in vitro* tissue capable of mimicking the depth dependent nanostructural organization of the fibrous collagen network of the native articular cartilage by combining biomaterials and cells with suitable fabrication techniques. In this way, it will be possible to simulate the biochemical, mechanical and morphological properties of the native articular

cartilage and consequently provide enhanced chondrogenic conditions able to solve problems as osteoarthritis [1,28].

2.2.1. Scaffolds

TE is a combined field of knowledge and technologies (in engineering, materials science, biology and biomedicine) that are meant to improve or replace natural/biological tissues by combining biomaterials, advanced micro fabrication techniques and cell culture strategies. Scaffolds can be used as support for cell migration, proliferation and differentiation, in order to promote tissue regeneration [29]. For cartilage TE purposes, an ideal scaffold should be capable to provide a comfortable 3D niche for the cells and stimulate them to synthesize cartilage matrix, enabling the replacement of the native matrix until the new cartilage is formed. These scaffolds should: a) be biodegradable, sterile, biocompatible and non-toxic; b) have a porosity that allows the diffusion of nutrients and waste products, support cell attachment, proliferation, differentiation and ECM production; c) have elasticity and give mechanical support; d) be able to mimic the anisotropic morphology and biochemical environment of the different zones [12,30].

Modern scaffolds are usually made of natural or synthetic polymers. Some examples of natural polymers include proteins (such as silk, fibrin and collagen) and carbohydrates (such as agarose, alginate, hyaluronan and chitosan), which can both be used to fabricate highly biocompatible hydrogels able to encapsulate chondrocyte cells without inducing dedifferentiation. These biomaterials have good biocompatibility, but lack strength and dimensional stability due to gelation and rapid hydrolysis in aqueous media [11,12]. Hence, collagen and elastin-based substances are, for example, unlikely for vascular TE [31,32].

On the other hand, synthetic polymers exhibit better strength and adaptability (are easier to tune) compared to natural polymers, but often do not allow cells to maintain their phenotype, leading to the production of ECM with different properties. Polylactic acid (PLA), polyglycolic acid (PGA), polylactic-co-glycolic acid (PLGA) and polycaprolactone (PCL) (Figure 5) are some examples of synthetic polymers [11,12].

So, the combination of both types of polymers is essential to the development of a scaffold capable of mimicking the biochemical composition of ECM, and at the same time, owning good mechanical properties [31,32]. This was shown by Ahmed *et al.* [33] when they combined collagen with synthetic polymers PLA and PLGA to develop a suitable 3D structure to grow chondrocytes with minimal dedifferentiation for cartilage repair. Also, the

fatigue levels of polyvinyl alcohol (PVA) gel filled PCL scaffolds were studied at different dynamic conditions by Vikingsson *et al.* [34] with up to 100,000 cycles of unconfined compression, and it was shown that the scaffolds were able to maintain their morphology and stress-strain response, withstanding the compressive forces and therefore, showing that it can be used for regeneration of new tissue. In other example, Hsu *et al.* [35] showed that the combination of poly(L-lactide) (PLLA) and PGA, modified with type II collagen, increased chondrocyte proliferation and higher glycosaminoglycans and collagen production.

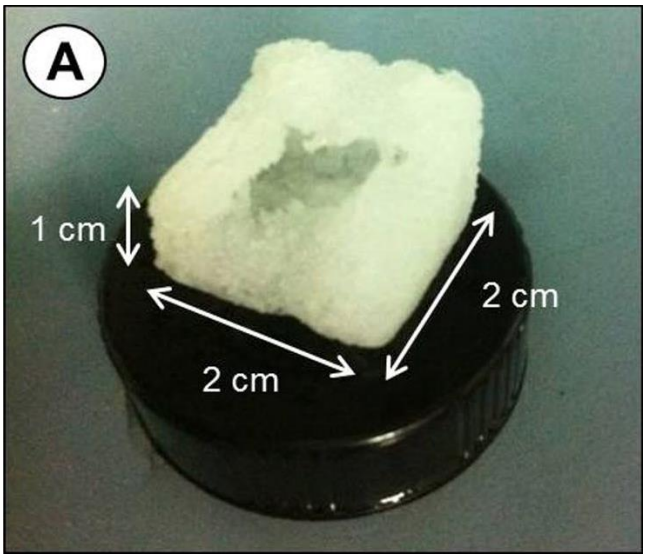

Figure 5 - Photography of a 3D synthetic polymer (PCL) microporous scaffold. Adapted from [36]

Additionally cartilage TE scaffolds can also be used in dynamic cell culture protocols, in order to predict their mechanical performance *in vivo* or/and to enhance cell response [37,38]. Indeed, several experimental studies using bioreactors concluded that appropriate mechanical stimulation can improve the mechanical properties of engineered cartilage [39]. For example, Spitters *et al.* have developed a bioreactor capable of combining cyclic mechanical loading and a nutrient supply similar to the cartilaginous microenvironment in order to modulate degenerative diseases [40]. In another work Jung *et al.* used mechanical stimulation of a 3D poly(lactide-co-caprolactone) to successfully enhance the chondrogenic differentiation of bone marrow stromal cells, boost the production of cartilaginous ECM and promote the maintenance of chondrocyte phenotype [41].

2.2.1.1. ELECTROSPUN NANOFIBROUS SCAFFOLDS

Electrospinning is a technique known for its affordability, simplicity, vast range of material selection, and high flexibility in controlling diameters and spatial orientation which enables the production of nanofibrous scaffolds (Figure 6) with potential for applications in TE and regenerative medicine [42]. Thus, in order to mimic the fibrillar network of articular cartilage, nanofibrous scaffolds made by electrospinning are composed of fibres with diameters on a nano scale, making them able to mimic the natural cell-ECM interactions and therefore promote the production of cartilage-like tissue to provide a new organized matrix [11,24].

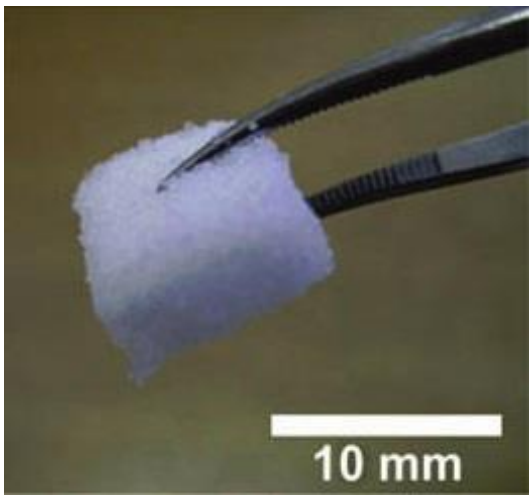

Figure 6 – Example of nanofibrous scaffold: homogeneous hyaluronic acid/collagen nanofibers and NaCl salts construct. Adapted from [42]

In TE, fibrous biomaterials present the most convenient architecture due to their high porosity, high surface volume ratio and topographic resemblance to the natural ECM [42]. The nanofibre scaffolds possess high specific surface area for cell attachment, allow oxygen permeability and prevent fluid accumulation making it also great for nutrient transport. An higher microporous structure and a 3D biomaterial contact for cell interaction, makes it possible to control cellular orientation and morphology in order to achieve the intended ECM architecture [31,43].

These scaffolds can be made through a layer-by-layer method, varying both fibre size and orientation (by changing polymer concentration, collection conditions and collector velocity to make fibres aligned or randomly oriented), rendering them suitable for making scaffolds capable of mimicking the different zones in articular cartilage and its properties (such has its organizational characteristic, the ability to successfully support cartilage

formation and its superior mechanical features) [2]. The fact that is possible to make aligned fibres is very advantageous, because it is ideal for cells that prefer some specific type of cues to grow and migrate [31].

2.3. Polycaprolactone (PCL)

Polycaprolactone (PCL) is a biocompatible and biodegradable material used for medical applications, drug delivery systems and packaging materials. PCL shows higher potential to prevent postsurgical adhesion and has more advantages over other synthetic polymers like PLLA, PAG, PLA and PLGA such as better mechanical strength, granting more stability under ambient conditions, being cheaper and available in large quantities, and being able to last long enough for cell proliferation before it's *in vivo* degraded, when compared to other synthetic polymers [44–46]

PCL is a semi-crystalline and hydrophobic polymer soluble in a wide range of organic common solvents and hydrolyses under physiological conditions into water-soluble monomers [47]. Indeed, the concentration of the polymer (solute), the type and concentration of the solvent actively determines the characteristics of the resulting meshes/scaffolds [48]. Also, it is a Food and Drug Administration (FDA) approved material, presents a very slow degradation rate (2–4 years depending on the starting molecular weight) and has been used as a slow release drug delivery device and suture material since the 1980s. PCL possesses a predictable and single low melting point (50-60ºC) and is characterized by its polarity and potential for hydrogen bonding, being lower than PGA and PLA. Also, its rheological and viscoelastic properties allow it to be used in a wide range of scaffold fabrication technologies. Due to these characteristics, it's use for scaffold fabrication is increasing within the TE community [49].

Yet, PCL has some limitations, its hydrophobic nature leads to decreased wettability of the surface which in turn disables the performance in cell adhesion, resorption and reproduction [44]. Also, PCL has poor mechanical strength for applications under load bearing conditions. In order to improve its mechanical properties, PCL can be combined with other materials, such as nanoparticles [45]. Actually the use of PCL combined with another material as a composite is very frequent, more than being used alone. A nanofibre composite scaffold was developed with PCL-graphene by Song *et al.* [50], proving that, besides having good mechanical properties (such as tensile stress and elastic modulus), it enhanced adhesion, differentiation and proliferation of mouse marrow

mesenchymal stem cells showing its higher biocompatibility if combined with other materials. In another study, electrospun PCL/GO-g-PEG structures (Figure 7) were studied for its structural and reinforcing effect. It resulted in improved tensile properties and the preliminary biological assay showed enhanced capability for supporting cell attachment and growth [51]. Also, as Zhang *et al.* [52] showed the possibility of combining PCL with other polymers, mainly gelatine, resulting in the development of a scaffold with better mechanical properties and favourable wettability, which in turn improved cell interactions, making it useful for applications in the biomedical field.

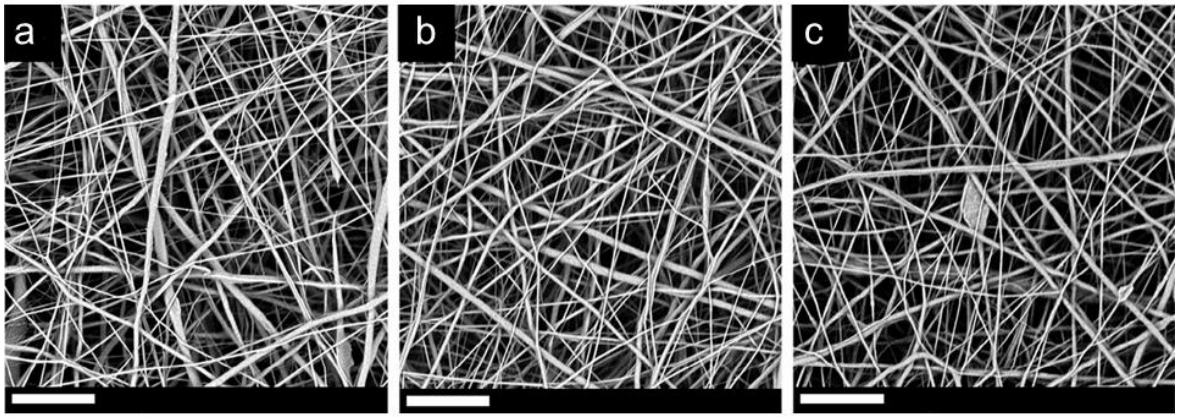

Figure 7 – Usage of PCL meshes combined with other materials (GO-g-PEG): (a) PCL/GO-g-PEG 0.25 wt%; (b) PCL/GO-g-PEG 0.5 wt%; (c) PCL/GO-g-PEG 1.0 wt%. Scale bars are 20 μm. Adapted from [51]**.**

PCL's capability for spinning allows its production in a fibrous form. Since it is an easy to use and cost effective, electrospinning is the most popular technique to fabricate fibrous PCL scaffolds (Figure 8) in order to be used in a broad range of biomedical applications [47]. Electrospinning is effective in producing ultrafine fibres with diameters ranging from microns to a few nanometres, by using an electric field to convert polymer solution into a fibre form. This happens due to stress created by applying electric current, creating a deformation of the droplet, which is ejected as a fluid jet that is elongated and collected in a collection device [52].

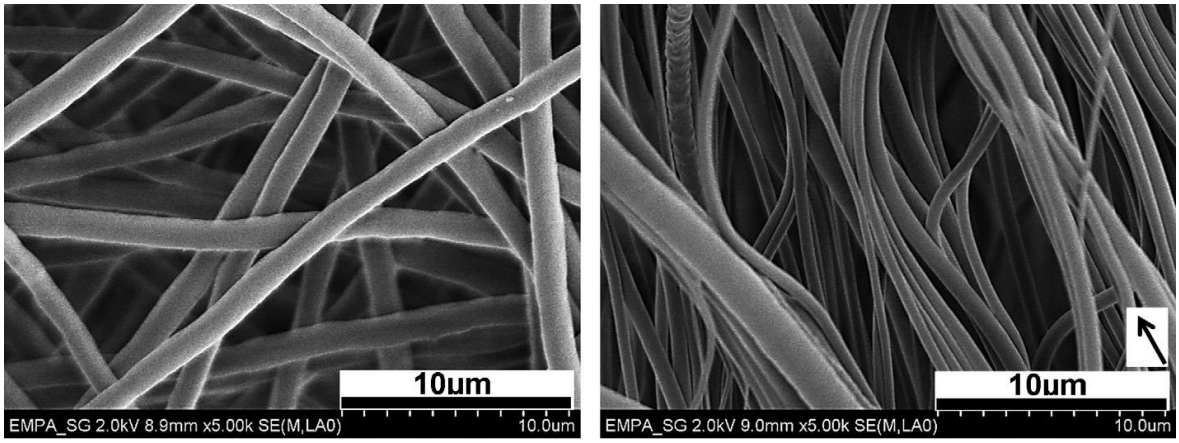

Figure 8 – Morphology demonstration of PCL nanofibers produced by electrospinning. Adapted from: [53]

2.4. Polycaprolactone Scaffolds in Tissue Engineering Applications

Recently, the use of PCL for scaffold fabrication has been increasing for biomedical applications, such as in the synthesis of complex biomaterials and TE. When making PCL electrospun-scaffolds it is important to know the factors that influence the cellular processes: fibre diameter, fibre alignment, elasticity, pore size distribution and porosity, surface topography and surface chemistry for improved cell-biomaterial interaction [49]. Dual fibrous structures composed of microfibers and nanofibers produced from PCL by wet electrospinning (which has a liquid collector instead of a solid one, in order to produce a bulky and fluffy material) are good to use as a scaffold. The fibres with bigger diameter have better mechanical properties and larger pore size (essential for three-dimensional cell distribution), while the fibres with smaller diameters are good for cell adhesion inside the scaffold [54].

Trilaminar fibrous scaffolds are important in order to mimic the morphological properties of articular cartilage. These scaffolds can support the production of cartilage-like extracellular matrix with depth-dependent organization, and this was achieved by McCullen *et al.* [2] by sequential electrospinning (Figure 9). Varying fibre size and orientation of PCL while changing polymer concentration and collection conditions, made possible the formation of zonally distinct cartilage layers. Their results showed that trilaminar scaffolds yielded higher tensile properties compared to fully aligned and randomly oriented fibres of the same or larger diameters. The trilaminar scaffolds

managed to get not only aligned cell morphologies in the superficial zone and spread in the randomly oriented in the deep zone of the scaffold, but they also enhanced a superior production of collagen type II.

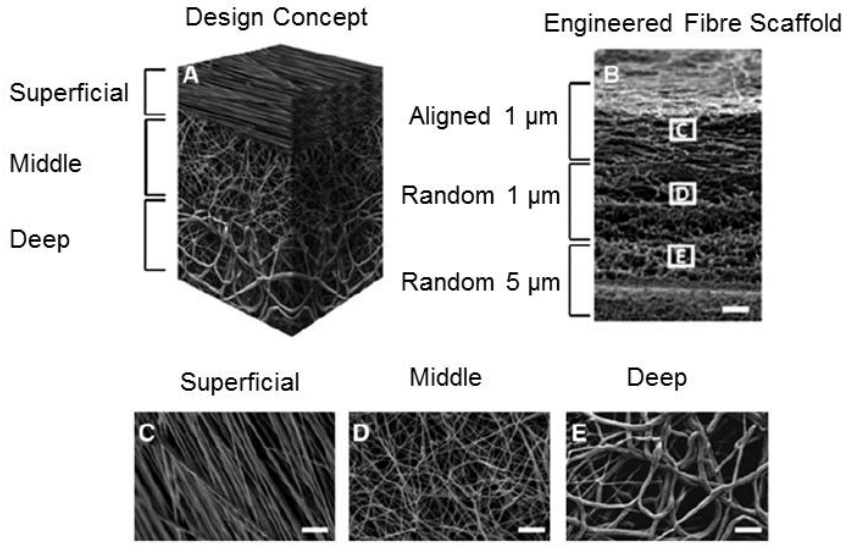

Figure 9 – Different concentrations and collecting conditions of sequential electrospinning of poly(e-caprolactone) were performed to generate dense fibres. (A) zonal placement of varying fibre zones; (B) resultant electron microscopy images of the bulk anisotropic scaffold; (C) aligned 1-mm fibres; (D) randomly oriented 1-mm fibres; (E) randomly oriented 5-mm fibres. Scale bar = 100 mm in (B) and 10 mm in (C–E). Adapted from [2]**.**

In other report, Steele *et al.* [55] have produced bilayered scaffolds (Figure 10) by electrospinning in order to mimic the functional interfaces and organization of articular cartilage. They noticed that their scaffolds demonstrated zone differences in cellular proliferation, biochemical composition and gene expression, proving that their results could be used in developing regenerative medicine strategies. They acquired these results by making a fibre zone composed aligned electrospun PCL on the surface of a PCL 3D porous structure. In another study made by Yang *et al.* [56], a scaffold consisting of fibrous PCL and methacrylated gelatine was conceived, which allowed the creation of a multi-layered structure tendon-like through photo-crosslinking of scaffold sheets. They tested this scaffold with human adipose-derived stem cells (ASCs) and noticed that the cells align along the orientation of the fibres and adopted tendon cell phenotype upon treatment with TGF-b3 growth factor, providing a mimic between the scaffold and natural tendon.

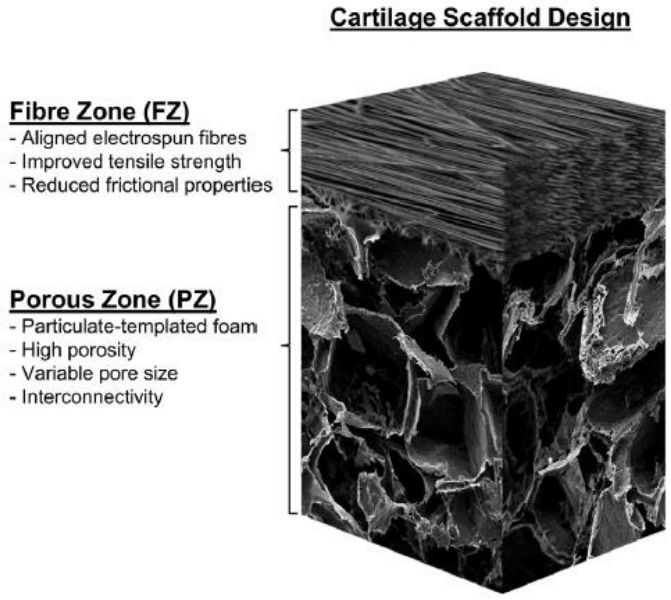

Figure 10 - Bilayered cartilage scaffold schematic. Diagram illustrating the electrospun fibre zone (FZ) deposited on a porous zone foam (PZ) forming an anisotropic scaffold. Adapted from [55]**.**

Li *et al.* [57] showed that 3D nanofibrous PCL were able to successfully support chondrocyte phenotype and matrix deposition (including collagen type II and IX). They achieved this mark by seeding foetal bovine chondrocytes cultured in medium with ITS+ (Insulin, Transferrin, Selenium), ascorbate and dexamethasone fibrous scaffold, that was able to recreate biomimetic characteristics, concluding that the PCL nanofibrous was suitable in scaffold biomaterials for cartilage TE applications.

The effects on mechanical properties of PCL could be enhanced by decreasing the fibre diameter, thus, improving the crystallinity, and by doing that, increasing the tensile strength and stiffness of the fibres, as shown by Wong *et al.* [58] when reducing the fibres to 700 nm.

When using a swine model to repair cartilage defects, Li *et al.* [59] produced a biodegradable PCL nanofibrous scaffold seeded either with allogeneic chondrocytes or xenogeneic human mesenchymal stem cells (MSCs) and compared them with an acellular PCL scaffold and a non-implant model. The difference was clear, the chondrogenic and MSC seeded scaffolds showed more complete repair when compared to the other two. Chondrogenic seeded scaffolds showed a fibro-cartilage like tissue, and the MSC ones showed hyaline cartilage like tissue. They also did a mechanical test showing that the highest equilibrium compressive stress was achieved by MSC-seeded scaffolds (1.5

MPA), followed by chondrocyte-seeded scaffolds (1.2 MPa) and the no-implant scaffold showing the lowest (0.2 MPa).

In complex cartilage TE strategies, electrospun nanofibers can be combined with hydrogels, which add to the topographic cues a three-dimensional environment for the cells that can also be loaded with growth factors, making it useful for repair of damaged cartilage, among other applications [60]. By adding an hydrogel to a PGA nanofibrous scaffold, Yang *et al.* [43] managed to develop an easy way to handle and apply composites with three nanofibre mesh layers and different internal orientations. Additionally, they managed to get human corneal fibroblasts to attach and proliferate in the different zones, and at the end of two days, cells replicated the nanofibers orientation (both aligned horizontal and vertical, and random-middle zone).

In another strategy, by using a perfusion reactor system, Silva *et al.* [61] managed to produce proliferation, support attachment and chondrogenic differentiation in bone-marrow mesenchymal stem cells by using electrospun PCL nanofibre meshes at a concentration of 17%, producing nanofibers with a thickness between 40-60 µm, 70-80% of porosity and an average pore size of 2.7 µm.

More recently an approach for tracheal TE was made by preparing a hybrid 3D scaffold based on PCL/Decellularized aorta (Figure 11). The mechanical properties, morphology, histology and also the outcomes of heterotopic transplantation in a rabbit were analysed. It was concluded that PCL maintained the rigidity of tissue engineered trachea when combined with the decellularized aorta and that it was suitable for tracheal TE due to its good mechanical properties, biocompatibility and cell adhesion [62]. Through the combination of PCL scaffolds embedded with europium hydroxide nanorods (EHNs), Augustine *et al.* [63] proved that the scaffolds with smaller weight percentage of the EHNs had increased tensile modulus and in *in vitro* studies they showed to have improved biocompatibility and cell adhesion properties. Also *in vivo* testing showed enhanced angiogenesis proving it could be used for TE applications.

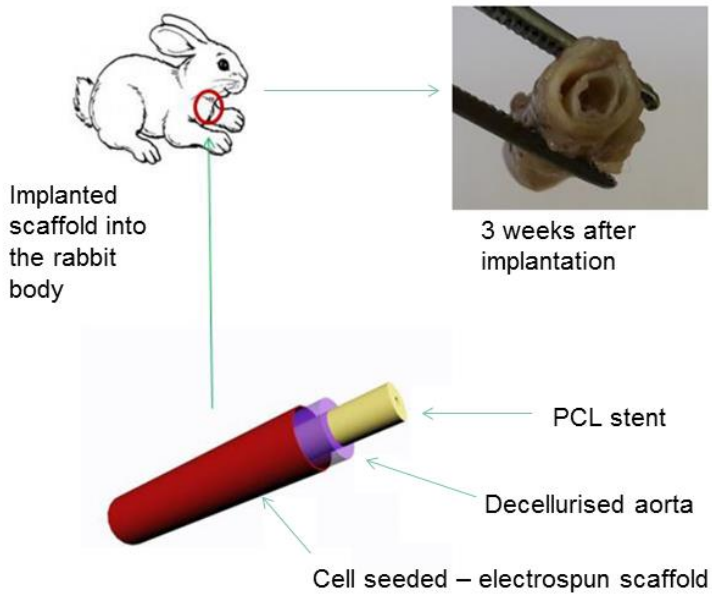

Figure 11 – Schematic representation of the tissue-engineered tracheal hybrid scaffold and its implantation. Three different types of electrospinning scaffolds based on PCL and collagen, were seeded by primary chondrocytes and adipose derived mesenchymal stem cells (AMSCs). The selected seeded scaffolds were attached to the acellular aorta, implanted into rabbit's muscle and harvested after 3 weeks. Adapted from [62]**.**

The combination PCL-PEG-PCL both as a scaffold/hydrogel (Ko *et al.*[64]) and as a film (Fu *et al.*[65]) demonstrated the ability for cells to manifest chondrogenic phenotype and produce cartilaginous ECM. In fact, the PCL-PEG-PCL film was implanted in rat knee defects and eight weeks after surgery, a new cartilage-like tissue was formed in the defect site, showing a grate capacity for repair of cartilage defects.

Graphene oxide and GO-polymer composites have been receiving special attention for its application in TE due to its biocompatibility and capacity for widely positive interaction and proliferation of different types of cells. A graphene oxide (GO)-poly (ε-caprolactone, PCL) scaffold was created to confirm its good biocompatibility and myoblast differentiation. The results proved the biocompatibility of the scaffolds, being a good candidate for tissue regeneration[66].

Taking everything into account, in this thesis it is presented four different anisotropic PCL fibrous architectures capable of combining fibrous and porous features in order to recreate specific 3D biomimetic microenvironments that are able not only to simulate the depth-dependent variations of each cartilaginous zone, but also to provide a

biocompatible and water retaining GO-collagen porous network suitable for cartilage TE protocols.

Chapter 3

MATERIALS AND METHODS

The starting point of the work described in this thesis was the conception and fabrication of an anisotropic tri-layered fibrous-porous PCL-GO-collagen scaffold developed by our research group through the on-going project “ARCADELIKE – DESENVOLVIMENTO DA ARQUITETURA FISIOLÓGICA DA CARTILAGEM DESENVOLVIDA IN-VITRO POR COMBINAÇÃO DE ESTÍMULO MECÂNICO E SCAFFOLDS FIBROSOS ANISOTRÓPICOS EM BIORREACTOR” (REF. PTDC/EMS-TEC/3263/2014). Therefore, this chapter will firstly describe the methods used for the design and fabrication of the original PCL-GO-collagen scaffold (3.1) in order to contextualize the work developed during the optimization of the porosity of the fibrous electrospun network (3.2), the fabrication and characterization of four different scaffold architectures (3.3) and the biocompatibility testing of the individual scaffold fibrous and porous components (3.4).

3.1. Scaffold Design and Fabrication

In order to recreate the 3D anisotropic fibrous structure of the cartilage, two different electrospinning methodologies (NANON-01A electrospinning machine) were used: towards making the superficial and the deep zones it was used a rotating fibre collecting device, which allows the alignment of the fibres; for the middle zone an ethanol (C_2H_6O) and water (H_2O) bath was used as the collector for the fibres in a random orientation (wet electrospinning). After that, the individual electrospun layers were assembled in the interior of a GO-collagen hydrogel and submitted through a lyophilization process to guaranty a biocompatible microporous porous structure capable of not only physically support the fibrous layers, but also improve the swelling properties of the overall system.

The GO-collagen hydrogel was fabricated according to [67]. Briefly, a GO aqueous dispersion with a concentration of 4 mg/mL (from Graphenea®) and a collagen solution

(collagen type I of rat tail in a concentration of 2.16 mg/mL in 0.6% of acetic acid (First Link Ltd) were mixed at pH = 2 with a 24 %w/w ratio col/GO , shaken for 10 seconds and centrifuged (Thermo Scientific™ Heraeus™ Multifuge™ X1 Centrifuge) for 10 minutes at 10 000 RPM.

3.1.1. Electrospinning Production of Fibrous Structures

To prepare the scaffold, the polymer PCL used presented a molecular weight of 80 000 Da, (Sigma Aldrich®). PCL was dissolved with a concentration of 12% in Dichloromethane and Dimethylformamide (Sigma Aldrich®) with a ratio of 8:2 (v:v) overnight while being agitated at room temperature.

For the production of the superficial and deep zones (Figure 12), the PCL solution was electrospun with a flow rate of 1 mL/h, a voltage ranging between 18-25 kV, a working distance (needle-collector) of 15 cm and a spinneret velocity of 5 mm/s. To ensure the fibres alignment, they were deposited during 5 hours on an aluminium foil that was fixed on the rotating collector device with a diameter of 10 cm and a speed of 2500 rotations per minute (RPM). The resulting electrospun mesh (approximately 100 µm of thickness) was then cut into 5 mm diameter cylinders. For the deep zone, rectangles with 2 mm width and 4 cm length were cut and rolled up into the shape of a spiral with 5 mm of diameter. This process occurred within a GO-collagen hydrogel in order to have the fibrous spiral branches intercalated with a micro-porous network after the process of lyophilization.

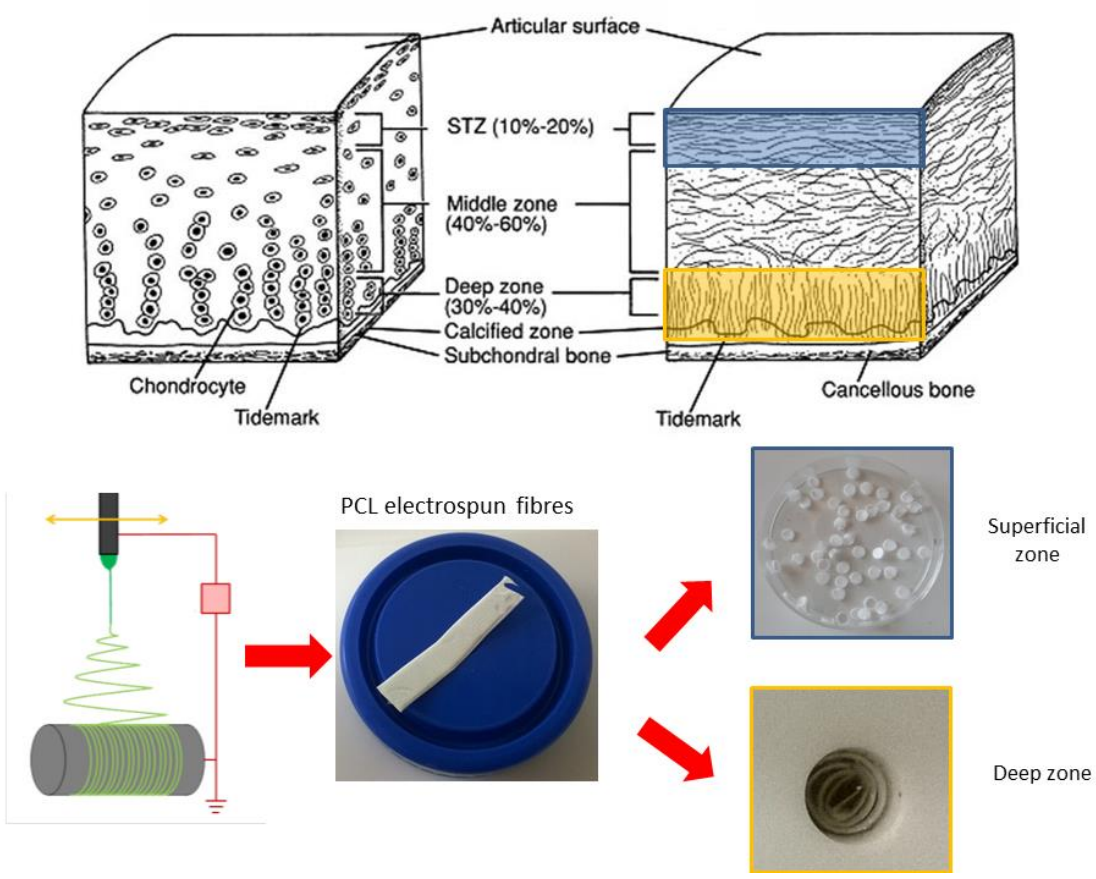

Figure 12 - Production of the superficial (blue) and deep zone (yellow). Natural cartilage scheme adapted from [9]

The middle zone was electrospun (Figure 13) with a flow rate of 1 mL/h, with a voltage between 20-30 kV, for a period of 30-40 seconds, using a 10 cm working distance between the needle and an ethanol:water bath in a ratio of 9:1 (v:v). The middle zone fibres were then placed into a cylindrical mould (5 mm of diameter and 2.5 mm of high) for shaping and stored in distillate water.

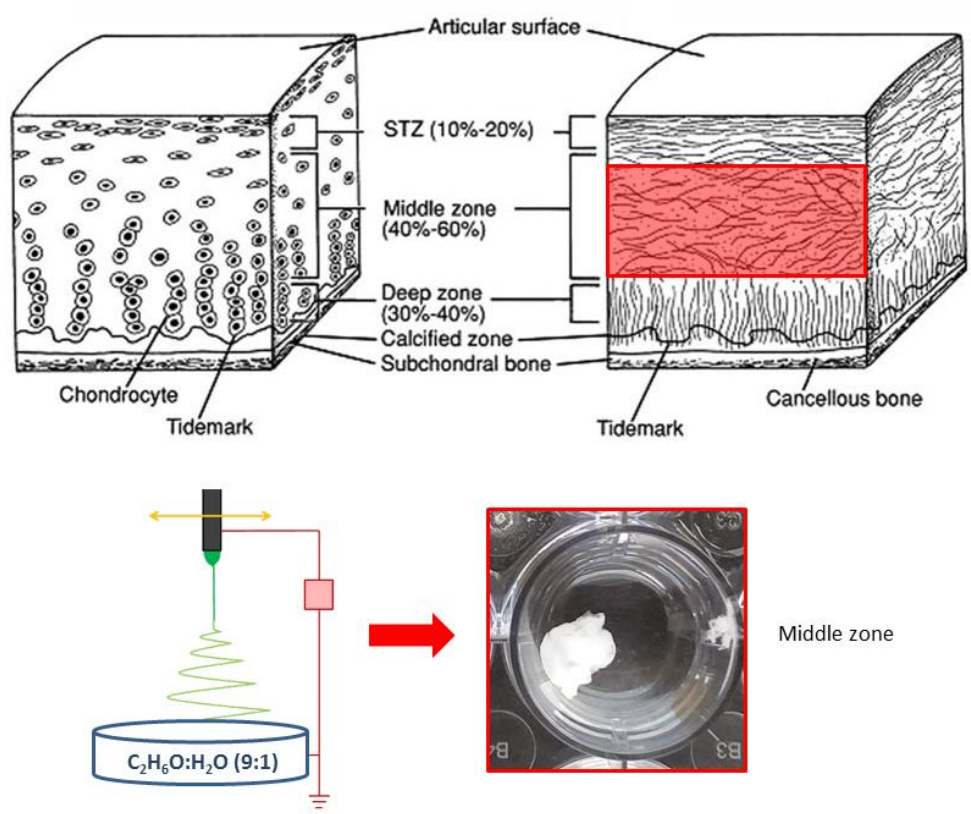

Figure 13 - Production of the middle zone (red). Natural Cartilage scheme adapted from [9]

3.1.2. PCL-GO-Collagen Scaffold Assembling

In order to assemble the scaffold, two moulds of Teflon were used, containing 6 cylinders each. Both moulds have 5 mm in depth but vary in the diameters of the cylinders: the first mould present cylinders with a diameter of 5 mm and the second have 10 mm of diameter (Figure 14). The mould with the smallest cylinder diameter was used to assemble the three different electrospun zones by combining the deep zone (5 x 2 mm), the middle zone (5 x 2.5 mm) and the superficial zone (5 x 0.5mm), which thickness was achieved by piling up the small electrospun cylinders. All the electrospun layers were previous immersed in ethanol and distilled water before assembly in order to sterilize them and remove the impurities. After assembly, the 3D electrospun structures were stored in the freezer at -20ºC for 4h.

Figure 14 - Mould 5x10 (left) and mould 5x5 (right)

After this period, the frozen electrospun PCL structures were placed in the mould with the biggest diameter, which was previously filled with the GO-collagen hydrogel.

Finally, the PCL-GO-collagen scaffolds were freeze-dried by lyophilisation (Telstar lyoQuest HT-40, Beijer Electronics Products) at -80 ºC in order to produce a complementary 3D fibrous-porous microenvironment (Figure 15).

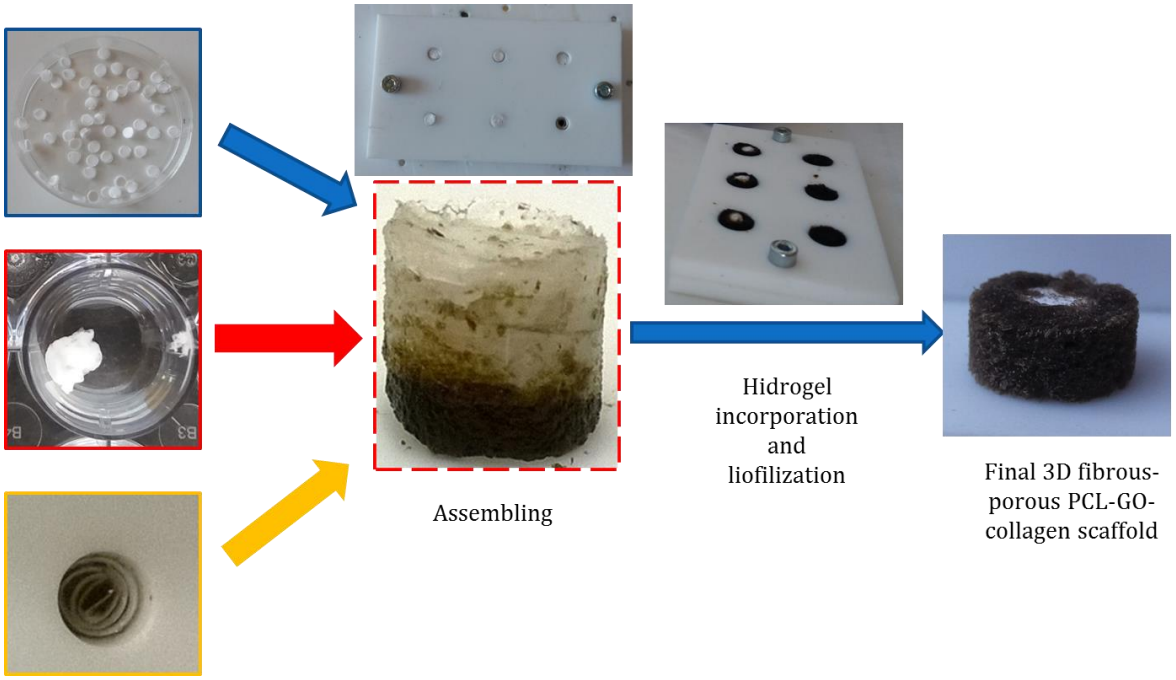

Figure 15 - Assembling process of PCL-GO-collagen scaffold. The superficial zone (highlighted in blue), middle zone (highlighted in red) and deep zone (highlighted in yellow) were put in the 5x5 mould. After being frozen, the 3D anisotropic fibrous structure were incorporated in the hydrogel on the 5x10 mould and submitted to lyophilization.

3.2. Optimization of Fibrous Structure Porosity

In order to enhance cell migration and proliferation for future cartilage TE applications, it was required to optimize the structure porosity of the scaffold according to the results acquired through previous work (Table 1). The goal was to achieve a large percentage of pores with a diameter superior to 10 μm.

Table 1 – Characterization of pore size and fibre diameter of the electrospun meshes developed previously by our group.

Superficial and Deep zones fibres		***Middle zone fibres***	
Fibre diameter	1.2 ± 0.5 μm	***Fibre diameter***	2.2 ± 0.3 μm
Average Pore size	2.6 ± 1.9 μm	***Average Pore size***	9.0 ± 4.4 μm

3.2.1. Optimization of Superficial and Deep Zones

Concerning to the optimization of the superficial and deep zones porosity, the velocity of the rotating collector device and the horizontal velocity of the deposition needle were altered. The other variables were maintained constant in all tests: solution concentration (12% PCL), flow rate (1 mL/h), spinneret width (30mm), voltage (25kV) and working distance (15cm).

The Table 2 summarizes the studied possibilities. Three different velocities were implemented on the rotating collector (25 RPM, 250 RPM and 2500 RPM) at a spinneret velocity of 10 mm/s and different spinneret velocities (1mm/s, 5mm/s and 10mm/s) at a rotating collector speed of 2500 RPM.

Table 2 - Different parameters studied for the optimization of the superficial and deep zone, highlighted with X.

	Collector velocity (RPM)		
Spinneret velocity (mm/s)	**25**	**250**	**2500**
1			X
5			X
10	X	X	X

3.2.2. Optimization of the middle zone

In regard to optimize the middle zone porosity the only parameter that was changed was the horizontal velocity of the deposition needle (0mm/s, 1mm/s and 10mm/s), while the others were maintained, such as the time of deposition (30s), voltage (20-30kV), solution concentration (12% PCL), flow rate (1 mL/h) and working distance (5cm).

3.3. Different Architectures

As soon as the fibrous structure porosity was optimized, four scaffold (PCL-GO-collagen) architectures were designed in order to study the influence of the fibre orientation in the mechanical properties and consequently the cell response. The scaffolds were made by adapting the described protocol (Chapter 3.1) to different architecture designs that will be described in section 3.3.1.

3.3.1. Architectures Description

Four architectures were chosen for the research. The selected architectures (Figure 16) were denominated as H1 (the three zones of the scaffold described in the process of assembling at 3.1.1), H2 (composed by the superficial and middle zones), H3 (composed by the superficial and deep zones) and H4 (composed of middle and deep zones). All four architectures were made and assembled in the same moulds and in the same conditions as previously described (3.1.1).

H2 architecture was made with a 2.5 mm height superficial zone, achieved by stacking electrospun cylinders with a thickness of 100 µm, and a 2.5 mm height middle zone.

H3 architecture was composed of a 2.5 mm height superficial zone and a 2.5 mm height deep zone. In order to acquire the 2.5 mm height deep zone, rectangles with 2.5 mm width and 4 cm length were cut and rolled up into the shape of a spiral with 5 mm of diameter within a GO-collagen hydrogel in order to make the spiral intercalated with a micro-porous layer after the process of lyophilization.

H4 architecture was built with a 2.5 mm height middle zone and a 2.5mm deep zone.

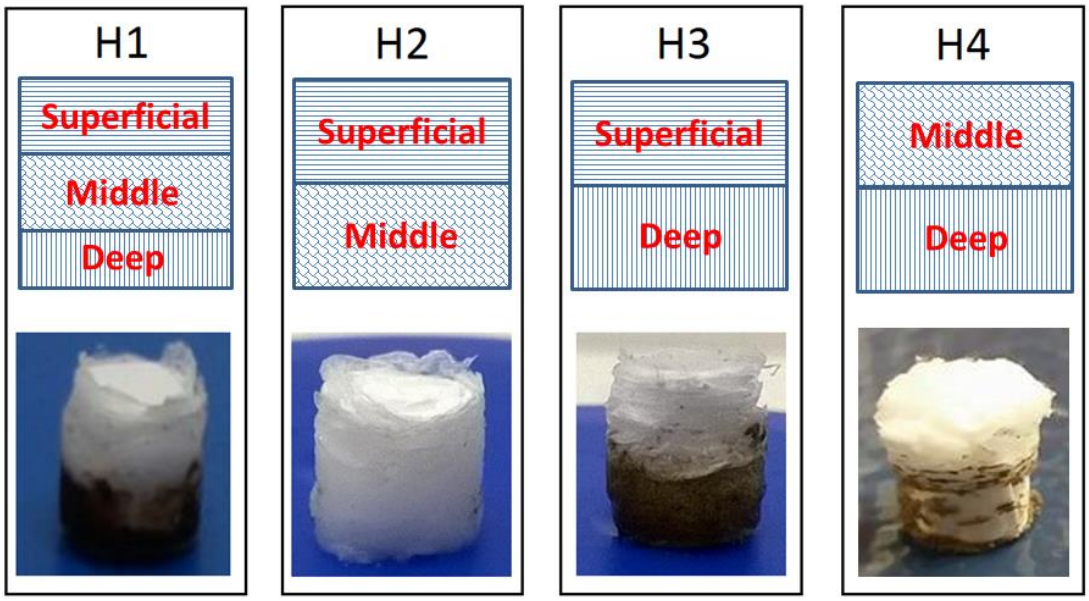

Figure 16 - Architectures description and design.

3.3.2. Mechanical and Topographic Characterization

The mechanical testing was done by using a Shimadzu MMT-101N (Shimadzu Scientific Instruments) (Figure 17) with a load cell of 100N. The compressive properties of the four different scaffold architectures were done in a wet state and they were compressed at a rate of 1 mm/min up to 15% of strain after a pre-charge of 0.07N. Although, the dimensions of the PCL-GO-collagen scaffolds tested were 10mm in diameter and 5mm in height, it was only considered a diameter of 5 mm since it was the right dimension for the interior fibrous structure of the scaffold. The compressive moduli of the samples were calculated through the study of the stress-strain curves calculated from the slope at low strain (0-15%). An identical methodology was applied for the three zones

when studied in separate, before the assembling into scaffold. The superficial zone samples had 5 mm diameter and 0.5mm height, while the middle zone samples had 2.5 mm height and 5 mm diameter and the deep zone samples had 2 mm height and 5 mm diameter. Also, it was studied the tensile properties for the superficial zone, using the same protocol previously described after the set-up of the machine was changed to study tensile modulus. For this test the superficial zone samples had 15 mm in height, 5 mm in width and with 250µm thickness.

The swelling properties were studied for the four different architectures and their structural resistance in water were evaluated by immersing the samples into distilled water at room temperature for a period of 24 h. The swelling ratio was calculated with the following equation:

$$Swelling\ ratio\ (mg/mg) = \frac{(W_s - W_d)}{W_d}$$

The fibres diameter and the pore size characterization of the three different zones (sections 3.2 and 3.3.2) were made through pictures taken with scanning electron microscope (SEM) (Hitachi SU 70; Hitachi High-Technologies Corporation, Krefeld, F.R., Germany) and analysed with the ImageJ software. The samples were fixed with carbon tape (Emitech K950 equipment) on the specific support for SEM and suffered sputter coating with gold (Au) in order to be analysed in SEM. At least 5 samples were used for each test.

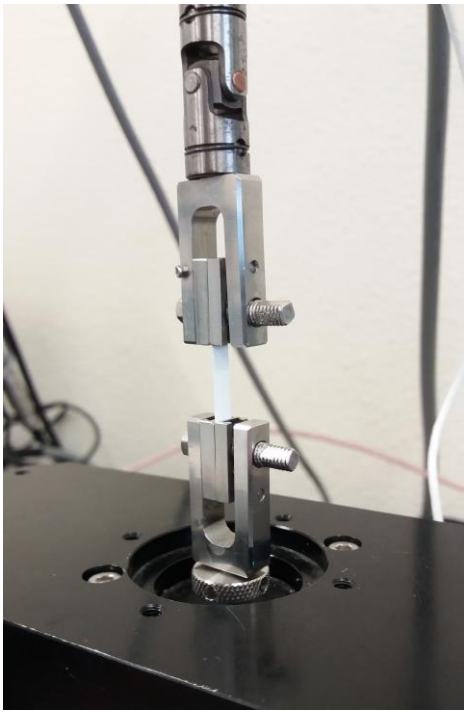

Figure 17 - Image taken of the Shimadzu MMT-101N mechanical testing machine while testing the tensile properties of a sample from the superficial zone.

3.4. Biocompatibility Testing

To start testing the biocompatibility of the PCL-GO-collagen scaffolds, the various components that make the composition of the scaffolds were first studied separately, each electrospun PCL zone and the hydrogel (GO-collagen) so that it could be possible to analyse the cellular response in each scaffold component. Cartilage progenitor cells were used and at determined time-points, samples were evaluated for cell metabolic activity and morphology.

3.4.1. Cell Expansion

The cells used for seeding the scaffolds were cartilage progenitor cell (Sigma Aldrich). These were the bovine (Bos taurus (Holstein-Fresian)) articular cartilage progenitor cell line that are able to re-differentiate into articular chondrocytes after extensive population doublings (>30 population doubling).

The cryopreserved cells were quickly thawed and cultured in 25 cm^2 tissue culture flasks containing Dulbecco's Modified Eagle's Medium/Nutrient Mixture F-12 Ham (Sigma-Aldrich), supplemented with 10% v/v inactivated foetal bovine serum (Sigma-Aldrich) and

1% v/v penicillin/streptomycin. Cells were maintained at 37ºC under a 5% CO_2 humidified atmosphere. The medium was refreshed every 3 days. Cells were harvested at pre-confluence using a 0.25% trypsin/EDTA solution and used in the passage seven.

3.4.2. Cell Seeding

Before cell seeding there were a few steps to consider in order to render the scaffolds to be suitable for cell proliferation. Scaffolds were sterilized in ethanol 70% for a period of at least 3 hours, washed with PBS three times (first for a period of 5 minutes, then 15 minutes and at last 30 minutes) and incubated with culture medium for 2 hour to promote the increase of cell attachment.

After this process, the scaffolds were ready for cell seeding. They were firstly seeded with 0,5 x 10^6 cells/scaffold and incubated for a period of 2 hours at 37ºC under a 5% CO_2 humidified atmosphere. Afterwards, culture medium was added until it reached a final volume of 1mL per well. The scaffolds were maintained in culture in the same conditions as cell expansion for 21 days and the medium was refreshed every 3 days. Positive (only cells) and negative (only scaffold) controls were used.

3.4.3. Cytochemical Staining of Actin Filaments and Nuclei

To have an idea of how, where and if the cells could infiltrate the scaffolds through all of its structure, a cytochemical staining of actin filaments and nuclei was used to visualize the cytoskeleton organization through the three different zones in separate for 1 and 2 weeks. After fixation with 4% w/v paraformaldehyde in PBS and permeabilization with 0.1% v/v Triton X-100, cells were stained for F-actin filaments (Phalloidin-iFluor 488; ABCAM) and for nuclei (4',6-diamidino-2-phenylindole, DAPI; Sigma-Aldrich) during 90 minutes in the dark at 37º C and then visualized using a fluorescence microscope (Axioimager M2, Zeiss) with magnification of 10x/0.25.

3.4.4. Metabolic Activity Measurement

The metabolic activity of the cells in the three different zones can be measured with the use of resazurin, a cell permeable compound that is blue in colour and non-fluorescent. When entering the cells, resazurin (dark blue in colour) is reduced to resorufin, a compound that is red in colour and highly fluorescent. The cells with viability will

continuously convert resazurin to resorufin, increasing the overall fluorescence and colour of the media surrounding the cells. The fluorescent or colorimetric signal generated from the test corresponds to the number of living cells in the sample. Then, by fluorometric or light absorption measurement, the amount of dye conversion in the solution is measured.

To avoid measuring cells attached to the well surface, scaffolds were transferred to a new 24 well plate. Then, a 10% (v/v) of resazurin solution (0.1 mg/mL in PBS) with medium was added to each well and incubated at 37°C between 1-5 h. Afterwards 100 µL per well was transferred to a 96-well plate and absorbance was measured at 570 nm and 600 nm using a microplate reader. The absorbance deduced for all the cell-seeded scaffolds was a result of the ratio optical density (OD.) 570/OD. 600 nm minus the OD. 570/OD. 600 nm ratio of a blank (resazurin media incubated in the absence of cells) and minus the OD. 570/OD. 600 nm ratio of a negative control (resazurin media incubated with the control scaffold).

3.4.5. Cell morphology visualization through SEM

As a complementary test to the visualization of cells done with the staining described in section 3.4.3, cell morphology visualization through SEM was made. This test was made to the superficial zone at the end of three weeks.

At the end of three weeks of culture in a 24 well culture plate, the chondrocyte seeded (0,5 x 10^6 cells/well) superficial zone was washed twice with PBS, fixed with 4% paraformaldehyde (PFA) for 30 minutes, and dehydrated through a gradient series of ethanol from 70% to 100% and dried. Prior to SEM (Hitachi SU 70; Hitachi High-Technologies Corporation, Krefeld, F.R., Germany) analysis, the samples were fixed with carbon tape (Emitech K950 equipment) on the specific support for SEM and suffered sputter coating with gold (Au) in order to be analysed.

3.4.6. Statistical Analysis

The values expressed for the resazurin measurement correspond to the mean ± standard deviation of five samples. The analysis of the ANOVA multiple values were used for the statistical analysis of the results in ORIGIN with the combination of the Turkey test. The value $p<0.05$ was considered as statistically significant.

Chapter 4

RESULTS AND DISCUSSION

4.1. Optimization of Fibrous Structure Porosity

As previously described (section 3.2) the PCL electrospun fibres for the superficial and deep zones had a diameter of 1.2±0.5 µm and an average pore size of 2.6 ± 1.9 µm. While the middle zone had a diameter 2.2 ± 0.3 µm and an average pore size 9.0 ± 4.4 µm. With the intention of optimizing the porosity and consequently enhancing cell migration and proliferation, a variation to the velocity of the rotating collector device and the horizontal velocity of the deposition needle were implemented for the fibres to be used as superficial and deep zones. For the middle zone, the horizontal velocity of the deposition needle was the only variable altered.

4.1.1. Optimization of Superficial and Deep Zones

When referring to the effect of RPM in the characteristics of the electrospun fibres (Figure 18) it is perceptible that the increasing of the collector velocity is directly proportional to the decreasing of the fibre diameter (50 RPM: 2.1 ± 0.3 µm; 250 RPM: 2.0 ± 0.4 µm; 2500 RPM: 1.1 ± 0.5 µm) and also in an increase of the number of pores with size <5 µm. Indeed it was expected that with a higher RPM, the fibres would have a bigger degree of alignment and therefore a smaller pore size when compared to lower RPM. The decisive aspect for choosing between 50 and 250 RPM was that, despite the slight difference between the produced fibres, at 250 RPM it was observed that the electrospun meshes had a bigger percentage of pores >10 µm making it more suitable for cell proliferation.

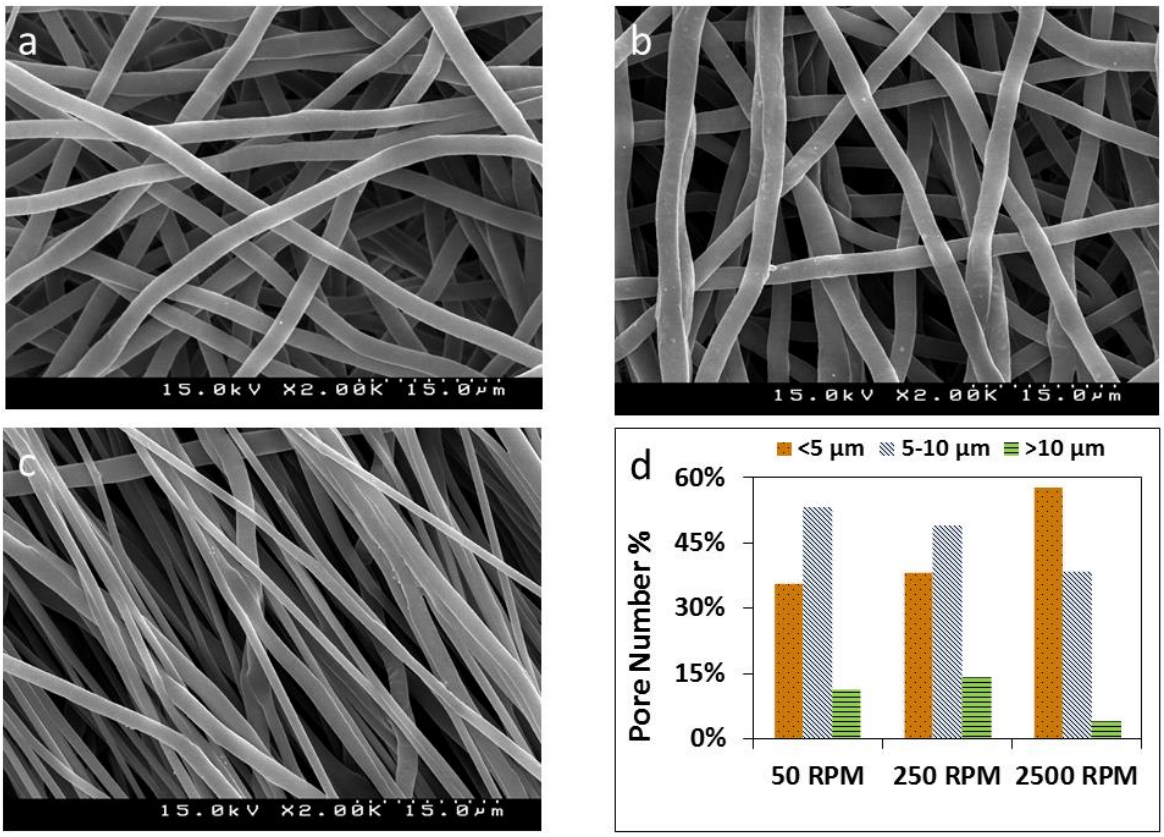

Figure 18 - Influence of the rotating collector device velocity on the topography of the electrospun meshes. Needle horizontal velocity = 10mm/s. (a) SEM image of 50 RPM fibres: diameter = 2.1 ± 0.3 µm; (b) SEM image of 250 RPM fibres: diameter = 2.0 ± 0.4 µm; (c) SEM image of 2500 RPM fibres: diameter = 1.1 ± 0.5 µm; (d) Pore size distribution (%) with influence of the rotating collector device.

In the case where the needle horizontal velocity was changed (Figure 19), there is no visible difference in fibre diameter that could have a significant impact (1 mm/s: 1.1 ± 0.5 µm; 5 mm/s: 1.1 ± 0.4 µm, 10 mm/s: 1.1 ± 0.5 µm). On the other hand at a lower velocity (1 mm/s) it is noticeable a bigger percentage of small pores (<5 µm), while the biggest percentage of big pores (>10 µm) was acquired at an intermediate velocity (5 mm/s). This result is justifiable with the fact that at this velocity it is possible to have a better distribution of fibres in the collector, avoiding the overlap of fibres registered at the lowest and highest velocity.

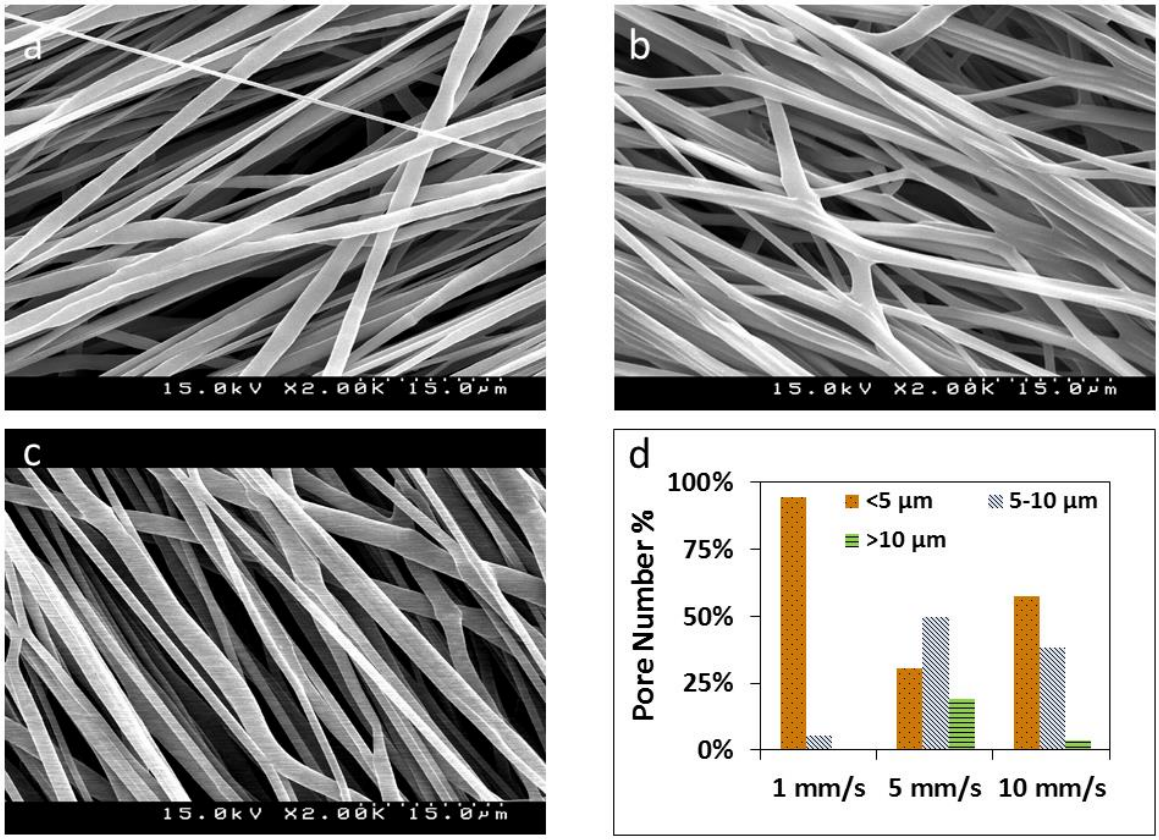

Figure 19 - Influence of needle horizontal velocity on the topography of the electrospun meshes. Rotating collector device velocity: 2500 RPM. (a) SEM image of 1 mm/s: fibre diameter = 1.1 ± 0.5 µm; (b) SEM image of 5 mm/s: fibre diameter = 1.1 ± 0.4 µm; (c) SEM image of 10 mm/s: fibre diameter = 1.1 ± 0.5 µm; (d) Pore size distribution (%) with influence of the needle horizontal velocity.

Therefore, the selected parameters for what was considered “optimal conditions” were a velocity of the collector device of 250 RPM and a needle horizontal velocity of 5 mm/s (Figure 20). In fact, when comparing the initial fibres (fibre diameter 1.2 ± 0.5 µm and an average pore size of 2.6 ± 1.9 µm.) with the ones produced in these conditions, it was acquired fibres with 1.3 ± 0.3 µm and an average pore size of 6.3 ± 1.9 µm, presenting around 85% of its pores equal or bigger than 5 µm. This numbers make these fibres more likely to induce proliferation and migration of cells due to bigger porosity when compared with the initial fibres.

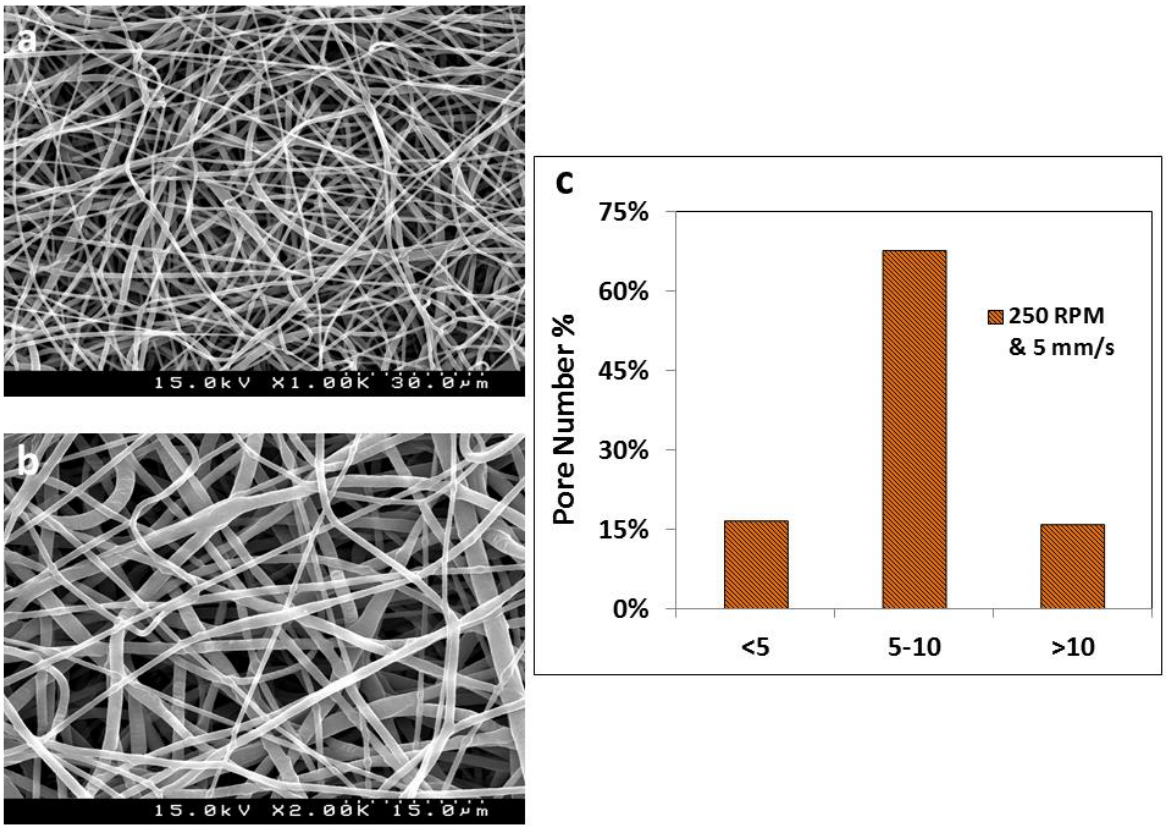

Figure 20 - Electrospun PCL fibres with optimal conditions (250 RPM and 5 mm/s). a) SEM image with scale of 30 µm; b) SEM image with scale of 15 µm; c) pore size distribution (%)

4.1.2. Optimization of Middle Zone

The horizontal velocity of the deposition needle was the only variable that was changed for the middle zone while trying to improve its porosity. The results did not show a significant alteration in the fibres porosity (Figure 21). Although at a spinneret velocity of 10 mm/s the fibres had a bigger percentage of pores with size >10 µm, the manual manipulation of the sample/fibres made it hard to collect fibres without damaging them. The percentage of pores with size <5 µm was almost the same throughout all the variations of speed. For these reasons it was chosen the 0 mm/s spinneret velocity which made the manipulation of the fibres easy and had a significant percentage of pores with size >10 µm. These fibres had a diameter of 2.2 ± 0.3 µm and an average pore size of 9.0 ± 4.4 µm

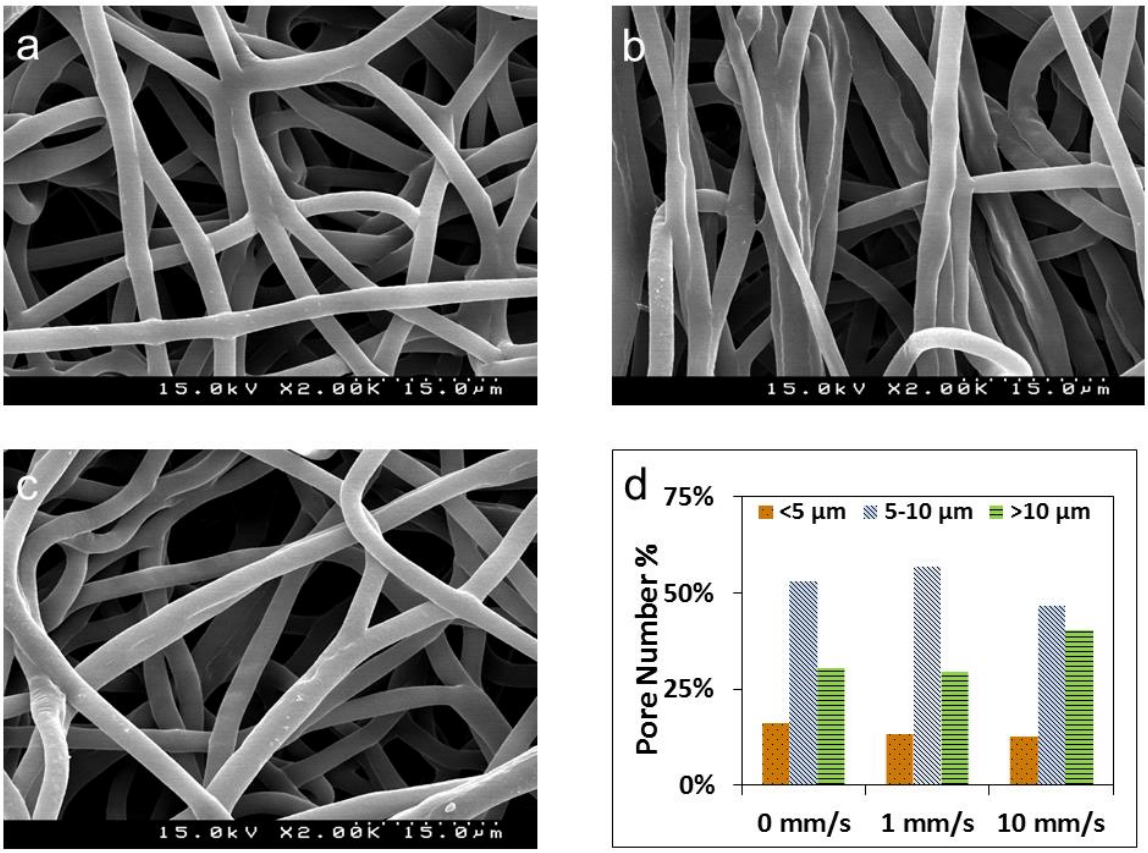

Figure 21 - Influence of needle horizontal velocity on the topography of the electrospun meshes. Images taken with SEM at scale of 15 µm. (a) 0 mm/s: fibre diameter = 2.21 ± 0.33 µm; (b) 1 mm/s: fibre diameter = 2.48 ± 0.61 µm; (a) 10 mm/s: fibre diameter = 2.29 ± 0.35 µm; (d) Pore size distribution (%) with influence of the needle horizontal velocity.

4.2. Mechanical and Topographic Analysis

As described in section 3.3, all the different electrospun zones (superficial, middle and deep) together with the four architectures were studied with the purpose of evaluating in which way the modifications in the fibres alignment and final depth dependent structure influenced the mechanical properties and therefore could impact the cellular response. In fact, the different anisotropic architectures had distinct mechanical properties due to their different topography. As expected it was possible to determinate the compressive moduli of each individual zone by calculating the slope of the typical linear region of the stress-strain curves (Figure 22a) [68–70]. Their respective compressive moduli and the superficial zone Young's modulus are presented in Table 3. The deep zone presents a lower R^2 (0.98 ± 0.01) than the other two electrospun zones (R^2 superficial = 0.982 ± 0.004 and R^2 middle = 0.982 ± 0.008) probably due to the fact that the fibrous branches of

the spiral are intercalated by a heterogeneous microporous GO-collagen network (Figure 23) [67]. It was considered 15% of strain in the three zones for the calculation of the compressive modulus because for all samples $R^2 > 0.95$ [2] and due to the fact that it was the limit of deformation from that the scaffolds totally recovered their initial height, which is a value compatible with the physiological properties of the native cartilaginous tissue [71,72].

In Figure 22b it is possible to compare the compressive moduli of all the three different zones. It can be concluded that the deep zone has the highest compressive modulus (164.46 ± 24.11 kPa) when compared to the other two zones (superficial = 27.33 ± 3.42 kPa and middle = 24.53 ± 8.49 kPa). This could be explained by the fact that, like in the natural cartilage, the deep zone presents fibres that are orientated vertically which could offer more resistance to the applied load. Also, if we compare to the natural cartilage, the deep zone is likewise the one which presents a higher compressive modulus [11]. When comparing the superficial and middle zone, they offer no significant difference between themselves. They do represent a lower compressive value when compared to Kim *et al.* [73] fibres which had a compressive modulus of 80 ± 20 kPa. The difference could be due to the fact that in this work it was used a flow rate of 1 mL/h and 30 s time of deposition, whilst Kim *et al.* used a flow rate of 2 mL/h and 10 minutes of deposition time, having a more dense final structure and enhancing its mechanical properties when compared to the ones in this study.

Figure 22c shows a representative tensile stress-strain curve ($R^2 = 0.99$) of the superficial zone. It showed a Young's modulus of 11.94 ± 1.14 MPa that, when compared to several bibliography showed to have a higher Young's modulus (3.7 MPa of 13% PCL [74]; 3.8 ± 0.8 MPa of 15% PCL [75]; 4.98 MPa of 10% PCL [52]). This could be explained by the rotation applied by the collector (at 1500 RPM), that the referred examples did not have (they were stationary). Indeed, the effect of the collectors velocity results in a better horizontal alignment of the fibres (and reduced pore size), which had the same direction as the force applied in the mechanical testing, culminating in an increased tensile modulus. For example, Thomas *et al.* [76] proved that a bigger rotation velocity of the collector improved the average tensile strength from 2.21 ± 0.22 MPa, at 0 RPM to 9.58 ± 0.71 MPa at 6000 RPM.

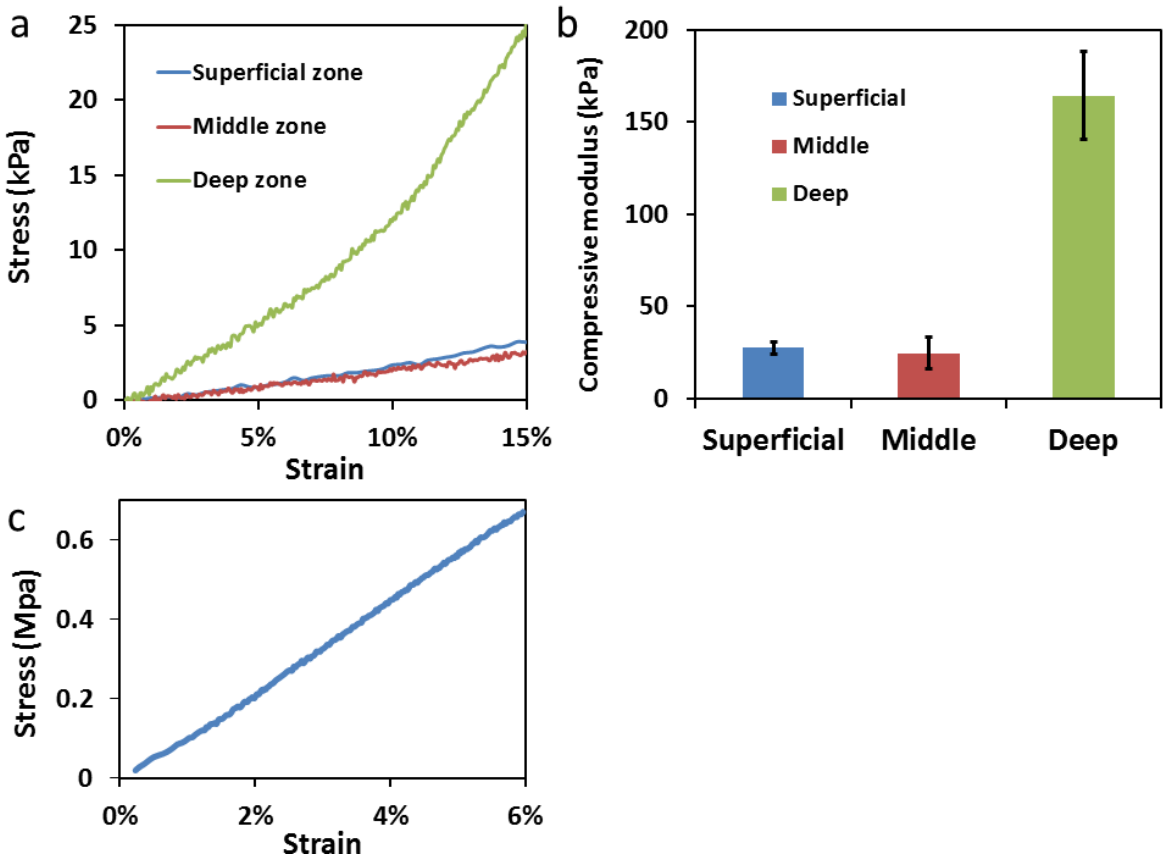

Figure 22 –Mechanical properties of the electrospun zones. (a) representative compressive stress-strain curves of the superficial zone (blue), middle zone (red) and deep zone (green); (b) compressive modulus of the three different zones; (c) representative tensile stress-strain curve of the superficial zone.

Table 3 - Compressive Modulus of the three different zones and Young's Modulus for the superficial zone

Zone	*Compressive Modulus (kPa)*	*Young's Modulus (MPa)*
Superficial	27.33 ± 3.42	11.94 ± 1.14
Middle	24.53 ± 8.49	
Deep	164.46 ± 24.11	

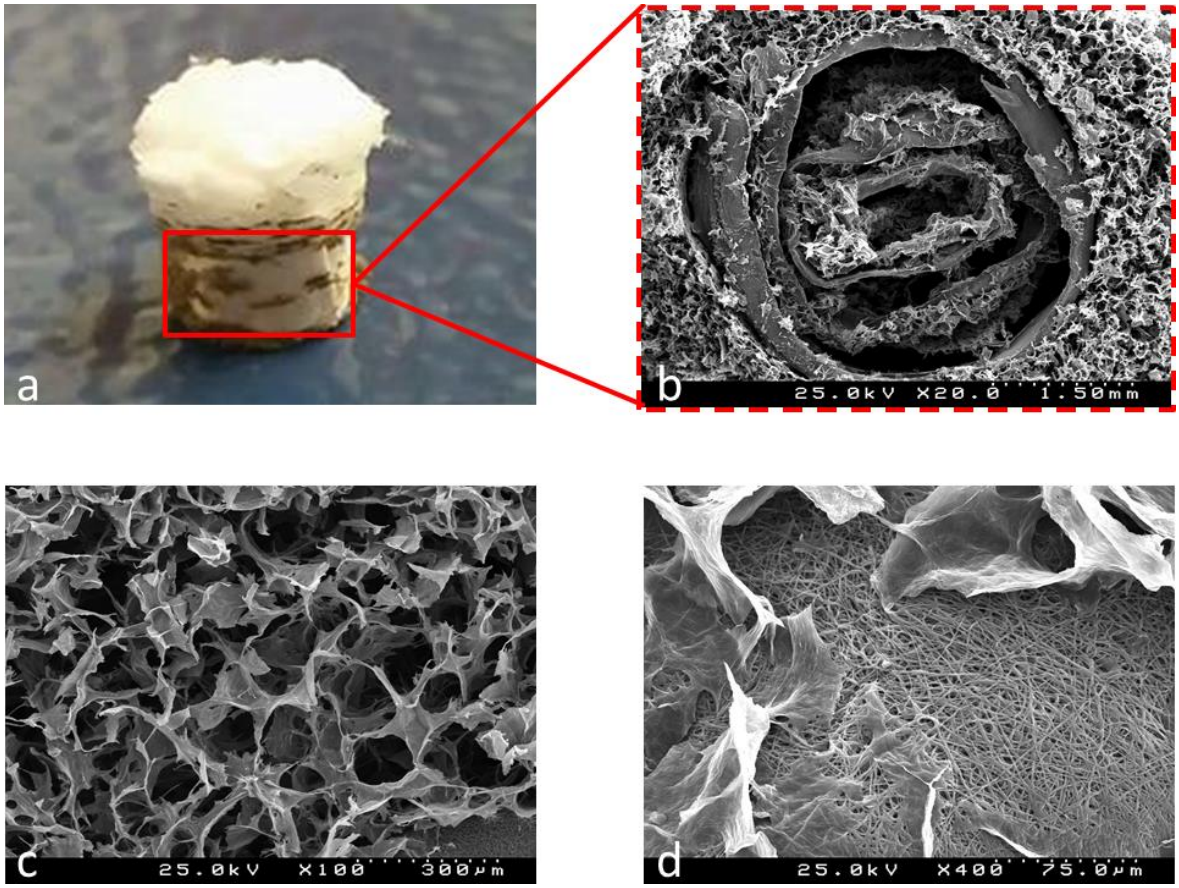

Figure 23 - (a) Architecture H4; (b) SEM image of the deep zone (spiral fibrous branches intercalated by a heterogeneous microporous GO-collagen network); (c) GO-collagen microporous structure; (d) GO-collagen microporous structure with the aligned PCL fibres.

The compressive moduli of the different architectures and their respective swelling ratio are presented in Table 4. When studying the compressive modulus of the scaffolds (Figure 24) it was observable that the architecture H1 (superficial+middle+deep = 38.07 ± 4.48 kPa) conferred a similar compressive modulus to the one of H2 (superficial+middle = 38.90 ± 3.06 kPa). One possible explanation for this is that the deep zone (that is presented in H1) has a compressive modulus that is much superior when compared to the other zones and therefore suffering less deformation. And since the deformation is only applied until 15%, it is not enough to see the mechanical response of the deep zone. For this reason, the compressive moduli of H1 and H2 are similar at 15% because essentially only represent the effect of the superficial and middle zone. This result reveals that the connection between the three zones in H1 must be optimized in order that the compressive modulus is not only affected by the superficial and middle zone, but by the three zones. One possible strategy is to establish chemical bonds between the PCL fibres of the three zones.

It is possible to conclude that the deep zone plays a key role in both the mechanical and swelling behaviour of the scaffolds. In fact, the architectures where the presence of the deep zone is more significant (H3 and H4 - 50% of the total high) present higher compressive moduli relatively to the other scaffolds (40% in H1 and 0% in H2). One possible explanation for the considerable difference between the compressive moduli of H4 (86.27 ±11.94 kPa) and H3 (60.12 ±11.31 kPa), which is surprising since the superficial and middle zones present similar compressive moduli, can be related with the superior swelling ability of the scaffold H4. In other words, as the middle and deep zones present respectively a larger fibre-fibre distance and a GO-collagen microporous network intercalated with fibrous branches, the scaffold H4 is more capable of retaining water comparatively with the scaffold H3, which in contrast presents a significant superficial zone with smaller pores. Consequently, it is possible that the larger amount of retained water contributes to a more efficient zone-zone assembly during the freezing process (Figure 15) and therefore to a more compact 3D structure.

When comparing the scaffolds compressive moduli values with the ones from natural articular cartilage, we can see that the scaffolds have lower compressive moduli since the natural cartilage, depending on the zone, could have compressive moduli of 1-19.5 Mpa [11,77]. This in turn has advantages and disadvantages. In one side, the inferior mechanical properties if meant to only promote initial engineered tissue growth in vitro, they don't require the level of mechanical strength of the natural cartilage. Since the scaffold will be meant to act as a supportive environment to help maintain the phenotype of the chondrocytes (which could be proved difficult) and therefore promote the formation of new tissue/ECM that then should withstand the same mechanical characteristics of the natural cartilage [78,79]. On the other hand, low mechanical properties could be directly affected by the degradation rate of the scaffold (the rate of scaffold degradation should be proportional to the rate of tissue formation to ensure sufficient mechanical support) [79]. As a solution, the implementation of mechanical stimuli through the use of a bioreactor, has been showed to improve the mechanical properties by increasing cell proliferation and ECM production guaranteeing the anisotropic distribution of collagen in engineered cartilage [24].

The swelling ratio showed no significant difference between the different architectures, proving that their capacity to retain water is slightly affected by the difference between the architectures (with the exception of H4 as previously described). The main influence in the swelling of the different architectures is probably due to the porous structure of the GO-collagen that is part of the final scaffold. Since PCL is a hydrophobic in its essence, the

retained water is mainly accomplished by the GO present in the scaffold that by nature has a high potential to store and adsorb water molecules due to the oxygen-containing functional groups on its hydrophilic surface [80–82].

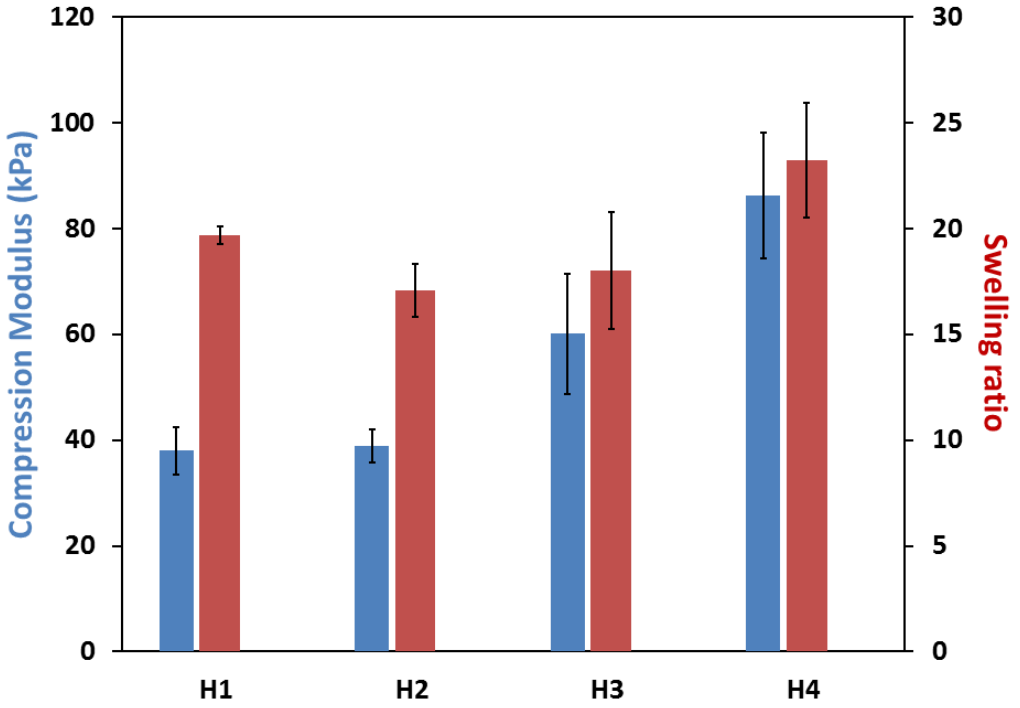

Figure 24 - Compressive modulus (blue) and sweeling after 24h (red) of the different PCL-GO-collagen scaffolds

Table 4 - Compressive Modulus and Swelling ratio of the different architectures

Architecture	*Compressive Modulus (kPa)*	*Swelling ratio*
H1	38.07 ± 4.48	19.71 ± 0.41
H2	38.90 ± 3.06	17.11 ± 1.25
H3	60.12 ± 11.31	18.03 ± 2.75
H4	86.27 ± 11.94	23.22 ± 2.71

4.3. Biocompatibility Testing

In order to characterize the scaffolds for their capability to sustain an environment for cells it was required the visualization of the cells nuclei and cytoskeleton through the staining of actin filaments, the SEM visualization of the cells presence in the superficial zone and the measurement of their metabolic activity.

4.3.1. Cytochemical Staining of Actin Filaments and Nuclei

The actin present in the cytoskeleton is determinant for chondrocyte shape which influences chondrogenic differentiation and ECM production, and it is by itself a signal for the presence of cells in the scaffolds [83]. To analyse the presence of the cells in the three different zones a cytochemical staining of actin filaments and nuclei was made. The images (Figure 25) were taken with a fluorescence microscope after 1and 2 weeks of culture.

The superficial zone revealed to be suitable for cells because it shows a large quantity of cells (nucleus in blue and the filaments in green) in its surface both at 1 and 2 weeks with no significant differences through time. This could be because the superficial zone is mainly 2D and in general way, 2D cultures are very suitable for all kind of cells, including chondrocytes. But the 2D kind of structure could also have limitations. If the cells don't infiltrate the scaffold and remain in a 2D structure they could: a) not provide the ECM structure of natural cartilage which is depth-dependent; b) make the chondrocytes lose their phenotype since it isn't taken to account the 3D natural cartilage structure and dedifferentiate into a fibroblastic-like morphology of chondrocytes that would lead to decreased ECM production, up regulation of collagen type I gene expression and down regulation of collagen type II gene expression [84–87].

At the first week, the middle zone presented big adherence for the cells since it is very noticeable their presence in its structure. But by the second week this changed drastically has it isn't possible to see a single cell in the structure. Some reasons can be pointed out for this result. The first is the manipulation of the samples by itself, as it was required to change the samples from well at the end of 1 week, which in turn could force the detachment of cells or a simple unnoticed error committed that could have killed the cells. Another one is the variability of the samples, since the manufacturing of the middle zone didn't allow complete control of the sample size as well as pore size. Chondrocyte size is difficult to define since they have a big variation in volume when in hydration state and could have cytoplasmatic processes of <8 μm [88]. Some report that chondrocyte size is

around 10-12 µm and that could get as large as 40 µm ([89]), others report 20 µm ([90]) and in more recent studies of osmolarity it was registered a cell volume of ~597 μm^3 ([88]). Because of this big variability in chondrocyte size and volume, and their response to hydration, and since the middle zone has a pore of 9.00±4.44 µm, the cells could have simply not had space to grow and infiltrate in the middle zone structure and detach from the structure and therefore not being visible.

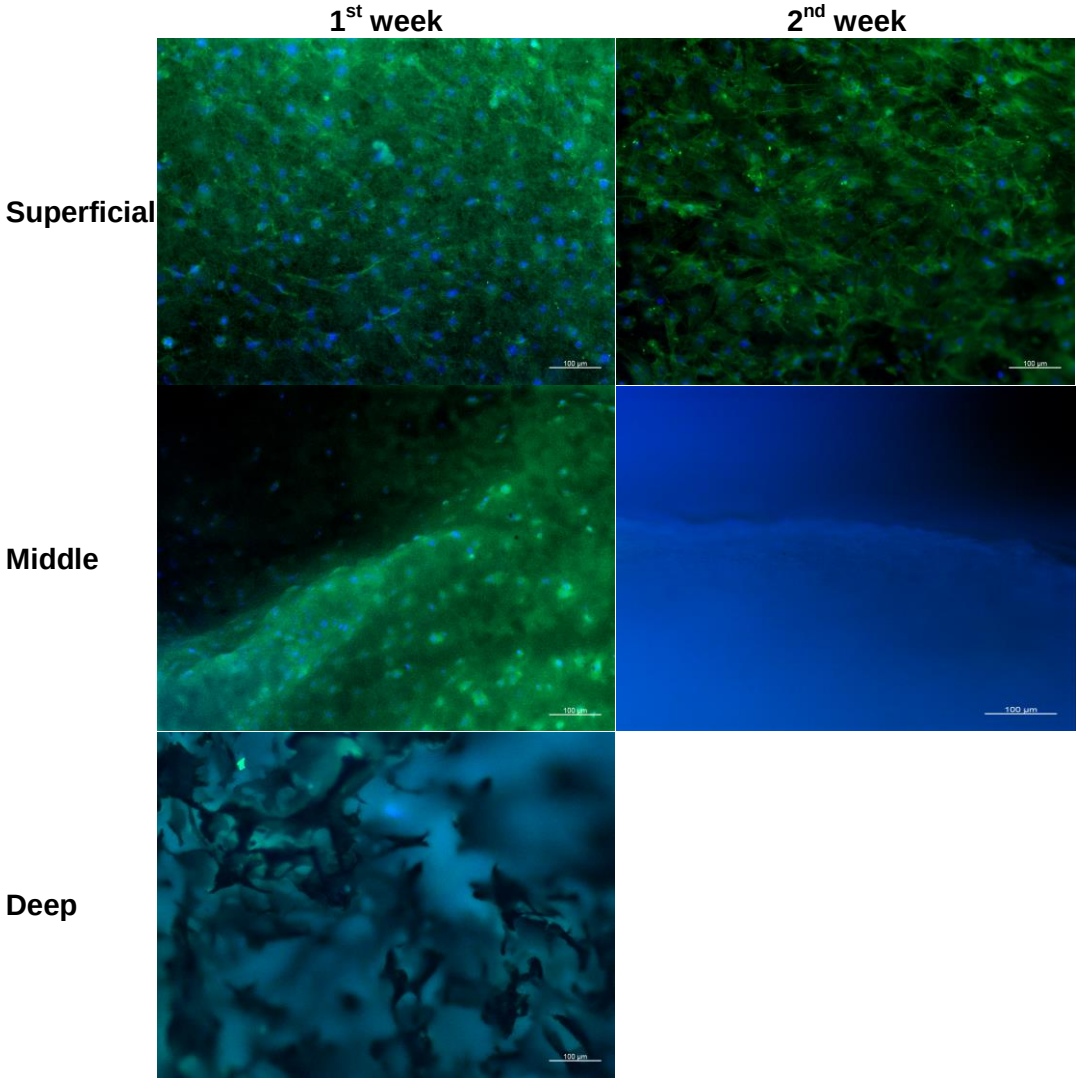

Figure 25 - Images taken with a fluorescent microscope with staining for actin filaments (green) and nuclei (blue) of the superficial, middle and deep zone after 1 and 2 weeks.

The deep zone presented a difficult structure to evaluate since it isn't possible to determine the presence of cells at the seventh day due to a problem of autofluorescence. Autofluorescence is when the material emits fluorescence signals that are difficult to be distinguished from the emitted signals of externally added fluorescence markers [91]. PCL is by itself autofluorescent, but comparing to the other zones pictures, it doesn't have a big

effect since it is still possible to see the cells. In the case of the deep zone, the problem stands with the GO. GO is an autofluorescent material, showing its autofluorescence through a big part of the emission spectrum: near-infrared, visible and ultraviolet [92,93]. A way to address this problem is to stain the samples with a labelling dye that has an excitation wavelength outside of the excitation spectrum of autofluorescent GO [91]. As the same problem would repeat itself at week 2, it was decided not to take the picture of the respective day.

4.3.2. Metabolic Activity Measurement

The metabolic activity of cells cultured in scaffolds and under control conditions was evaluated by the resazurin metabolism assay. The cells, when metabolically active, induce the reduction of resazurin to resafurin, inducing a chemical change from blue to a red colour. The metabolically active and proliferating viable cells will be proportionate to the resazurin reduction obtained [94,95]. It is a precise, simple and quick method which is non-cytotoxic and does not require the death of cells, making them viable for reuse for further investigations [94,96]. The results are shown in Figure 26 for the metabolic activity after 1 week, 2 weeks and 3 weeks.

In the first week, the superficial zone was the one that showed more metabolic activity and therefore had more cells residing in its structure when comparing to the others. This is probably due to the already explained fact of the 2D structure of the superficial zone, which is excellent for cell proliferation. The middle zone is the second to present high metabolic activity, followed by the deep zone and the GO-Collagen scaffold. The GO-Collagen scaffold presented a low value probably due to the special characteristic of GO. GO biocompatibility is very dose-dependent, as well as dependent from its physicochemical properties (size, surface charge, particulate state, surface functional groups and residual precursors), influencing the biological/toxicological activity [97,98]. It has been demonstrated by Wang *et al.* [97] that below 20 µg/mL GO had low cytotoxicity and that above 50 µg/mL it showed to be cytotoxic, leading to low survival rate, inducing cells to float and cell apoptosis and even providing organ failure and turning deadly when injected in mice at certain doses. This effect was increased as the time passed, causing increased cytotoxicity and leading to more apoptosis. It was registered that GO could internalize the cells to its nucleus, disturbing cell metabolism and gene expression by creating reactive oxygen species (ROS) [97–99]. For these reasons, the GO-Collagen scaffold probably presented less affinity for cells. Another explanation for these low values

could be the loss of structural stability of the GO-Collagen scaffold due to its degradation proving its highly dispersible characteristic in media due to the presence of oxygenated functional groups [99], that perhaps leads to cell detachment. This effect could be exacerbated by the scaffold manipulation during culture time. This behaviour can be also observed in the deep zone because it also contains GO-Collagen in its structure for maintaining its form.

In a general way it is possible to see that for the superficial and middle zone there is a slight decrease in metabolic activity throughout the weeks [the value verified for the middle zone at the third week is significantly lower than the values at the first and second week; the value verified for the superficial zone at the first week is significantly higher than the other values verified at the second and third week; according to the statistical analysis], possibly due to PCL current physical structure (pore size and distribution and fibre size) or for its chemical structure (making it hydrophobic) they could start to detach and adhere to the well surface or start dying at some point in time. A solution for this could be the functionalization of PCL with other substances (for example adhesion proteins) or materials (other polymers) to increase cell adhesion [100].

Although the middle zone visually presents higher metabolic activity than the superficial zone at the second week, the difference is not statistically significant. This gets in conflict with the results from the cytochemical staining obtained in this study, where we can see that there is no presence of cells in the second week in contrast to the superficial zone. This only reveals the big variability of the samples, which could make some samples more suitable as an environment for cell proliferation then others.

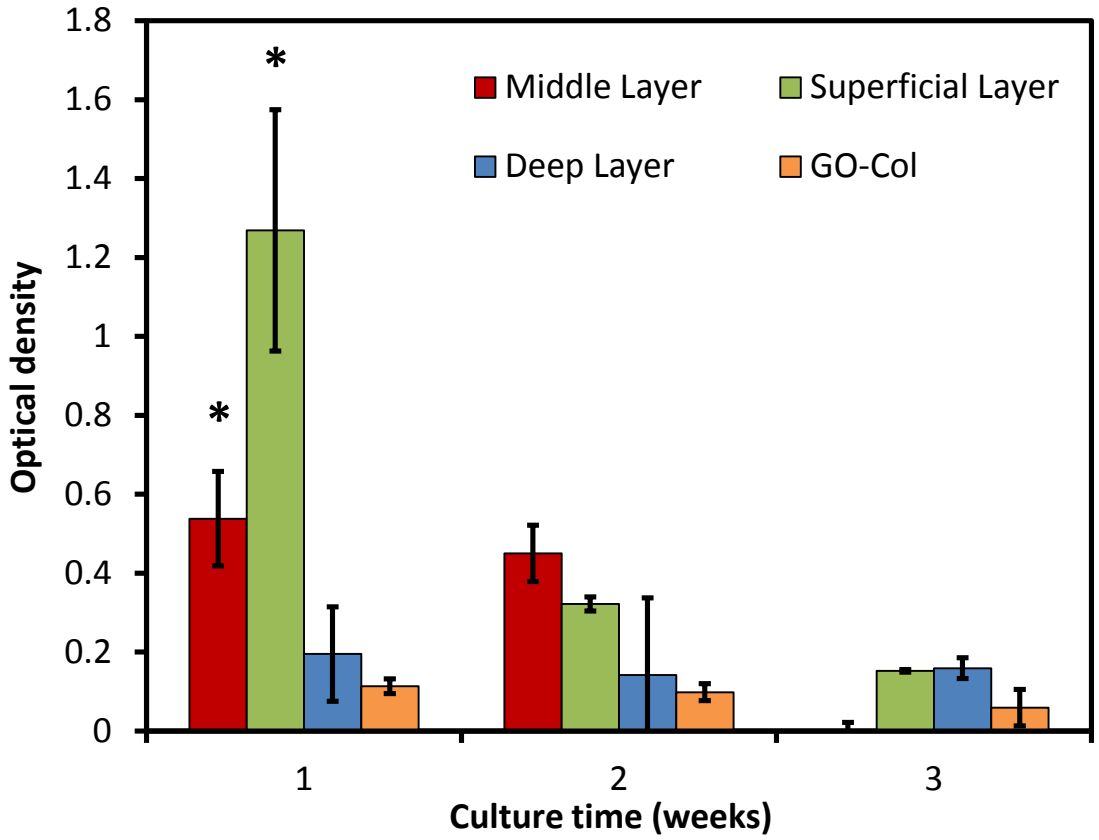

Figure 26 - Metabolic activity of the cells in three different zones (superficial = green, middle = red and deep = blue) and as control a GO-Collagen scaffold. The asterisk (*) represents the statistical significant differences ($p<0.05$).

4.3.3. Cell morphology visualization through SEM

As a parallel test to the staining of the actin and nuclei of the chondrocytes, it was proceeded a visualization of the cells morphology in the superficial zone using SEM. In Figure 27 it is possible to see with different scales (at 20 µm, 30 µm and 100 µm) and after three weeks of culture the presence of chondrocyte cells attached and spread to the surface of the superficial zone. They appear to be flattened and have their cytoplasmatic projections prolonging the cells body. This proves that the superficial zones were capable of sustaining cells after that period of time, and maintain a typical cell morphology [101].

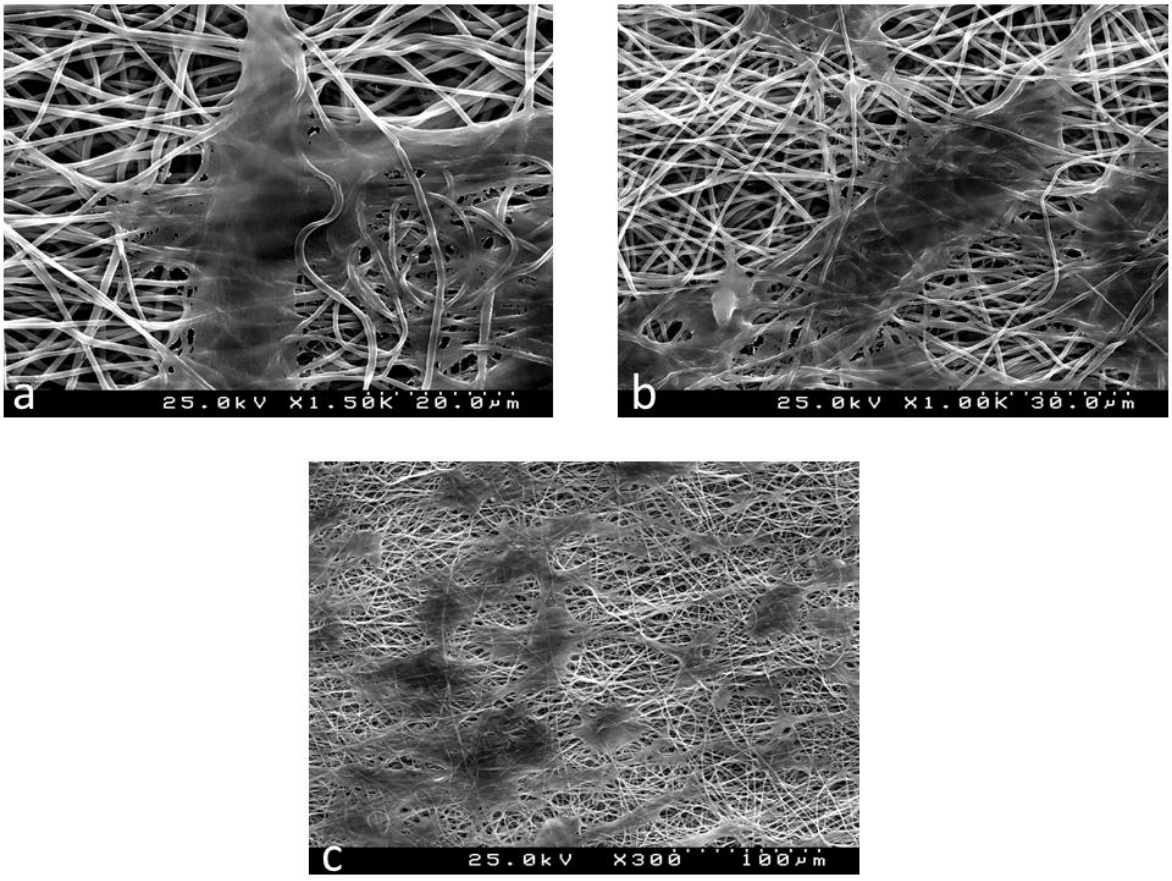

Figure 27 – Morphology visualization of chondrocytes cells in the superficial zone using SEM. (a) scale of 20 µm; (b) scale of 30 µm; (c) scale of 100 µm;

Chapter 5

CONCLUSIONS AND FUTURE WORK

5.1. Conclusions and Future Work

As initially intended, the optimization of the pore size for the three different zones was accomplished. For the superficial and deep zone the optimization led to a bigger percentage of pores with diameter superior than 10 µm. The middle zone optimization revealed that the previous electrospinning procedure (with the spinneret in static position) was the one to choose because it showed suitable pores and the final 3D electrospun zone was easier to manipulate when compare to the other options (spinneret velocity of 1 mm/s and 10 mm/s).

In the same way, the construction of four different anisotropic structures was successful and the mechanical tests revealed that the deep zone presented a higher compressive modulus when compared to the other two zones, which goes in agreement with the mechanical properties of natural cartilage. Indeed, the scaffolds that presented deep zones in their fibrous architectures had higher compressive modulus. The compressive modulus of the scaffolds is also influenced by the presence of the GO-collagen porous network due to its capacity to retain water. Although the mechanical features of all the PCL-GO-collagen scaffolds presented values compatible with cartilage tissue engineering protocols, it was also suggested that the deformation applied to the scaffold is sometimes not uniform, which requires consequently a way to connect the several zones of the scaffolds through PCL. One solution could be to establish chemical bonds between the zones of electrospun PCL. The scaffolds showed less mechanical properties than the natural cartilage which is somehow beneficial if it is only intended to seed the cells and have them proliferate and produce ECM. Additionally, the implementation of mechanical stimulation during cell culture could theoretically improve the mechanical properties of the scaffold.

Although having good results in a general way, the manipulation of the different zones that make up the scaffold are yet to be optimized since apparently they don’t allow the

chondrocytes cell culture to run in an efficient way. The seeding technique should also be optimized in order to enhance the contact between the cells and the scaffold

As it was observed, the superficial zone presented the best results in terms of cell proliferation and adhesion, but the pore size was still insufficient for allowing cellular migration, which is also noticeable in the other two zones. As a result of that, there is a need to optimize the fibrous structure porosity in order to have a pore size that could provide cellular migration and infiltration in the structure of the scaffolds in order for them to be functional. The preliminary biocompatibility evaluation shows high dependence on the optimization of the different zones in order to improve the accomplished results, through possible optimization of pores size and/or functionalization of the PCL with substances like adhesion proteins, in order to have more cells proliferating and thriving in the structure. If the cells have conditions to seed in a satisfying way and are able to proliferate and produce ECM, they will contribute for the maintenance and a better mimicking of the natural articular cartilage like microenvironment.

It should be done further degradation tests of the GO-collagen porous structure in order to evaluate if the current concentration of GO that is used in the construction of the scaffolds is causing any type of cytotoxicity for the cells.

REFERENCES

[1] T.J. Klein, D. Ph, J. Malda, D. Ph, R.L. Sah, D. Sc, D.W. Hutmacher, D. Ph, Tissue Engineering of Articular Cartilage with Biomimetic Zones, vol. 15 (2009).

[2] S.D. Mccullen, A. Callanan, E. Gentleman, M.M. Stevens, Anisotropic Fibrous Scaffolds for Articular Cartilage Regeneration, vol.18 (2012).

[3] A.J. Nóbrega, Development and production of anisotropic fibrous scaffolds with depth-dependent variations in the fibrillar size and orientation for cartilage tissue engineering. Master Dissertation - University of Aveiro, (2016).

[4] I.A. Olumegbon, A. Oloyede, I.O. Afara, Near-infrared (NIR) spectroscopic evaluation of articular cartilage : A review of current and future trends. Applied Spectroscopy Reviews. vol. 52 (2017).

[5] J. Schneevoigt, C. Fabian, C. Leovsky, J. Seeger, M. Bahramsoltani, In Vitro Expression of the Extracellular Matrix Components Aggrecan , Collagen Types I and II by Articular Cartilage- Derived Chondrocytes, (2016) .

[6] B. Johnstone, M. Alini, M. Cucchiarini, G.R. Dodge, D. Eglin, F. Guilak, Tissue engineering for articular cartilage repair – the state of the art, (2013).

[7] A. Aszodi, J. Roths, Microindentation Sensor System Based on an Optical Fiber Bragg Grating for the Mechanical Characterization of Articular Cartilage by Stress-Relaxation, Sensors and Actuators B. (2017).

[8] J. A. Buckwalter, H. J. Mankin, A. J. Grodzinsky, Articular Cartilage and Osteoarthritis. AAOS Instructional Course Lectures (2005).

[9] A. J. S. Fox, A. Bedi and S. A. Rodeo, The Basic Science of Articular Cartilage : Structure, Composition, and Function. Sports Health. vol. 1 (2009).

[10] G.P. Concaro S., Gustavson F., Bioreactors for Tissue Engineering of Cartilage, vol 112. (2009).

[11] P. D. Tatman, W. Gerull, *et sal.*, Multi-scale Biofabrication of Articular Cartilage: Bioinspired and Biomimetic Approaches, (2015).

[12] Ľ. Danišovič, I. Varga, R. Zamborsky and D. Böhmer The tissue engineering of articular cartilage : Cells , scaffolds and stimulating factors. Experimental Biology and Medicine (2012).

[13] R.J. Garfinkel, *et al.*, Vitamin D and Its Effects on Articular Cartilage and Osteoarthritis, (2017).

[14] U.R. Goessler, K. Hörmann, F. Riedel, Tissue engineering with chondrocytes and function of the extracellular matrix (Review), (2004).

[15] P. V. D. Kraan, C. Matta, A. Mobasheri, Age-Related Alterations in Signaling Pathways in Articular Chondrocytes : Implications for the Pathogenesis and Progression of Osteoarthritis – A Mini-Review, (2016).

[16] S. Camarero-Espinosa, B. Rothen-Rutishauser, E. J. Foster and C. Weder, Biomaterials Science Articular cartilage : from formation to tissue, (2016).

[17] S. Alina, S. Skrzyński, K. Śmiechowski, A. Kołodziejczaka, The review of versatile application of collagen, (2017).

[18] P. M. Kukkar, A.D. Savkare, M. R. Bhavsar and V. D. Gholap, A review on nanoparticle cross-linked collagen shield for sustained delivery of drug in glaucoma. College of Pharmacy, Nashik, Maharashtra, India. vol. 8 (2017) .

[19] S. Kuttappan, D. Mathew, M.B. Nair, International Journal of Biological Macromolecules Biomimetic composite scaffolds containing bioceramics and collagen / gelatin for bone tissue engineering - A mini review. Int. J. Biol. Macromol. vol. 93 (2016).

[20] T.S. Basale, S. Spinosum, S. Granulo-, S. Corneum, The Structure of Collagen within Parchment – A Review, (2003).

[21] T. Ariga, T. Miyatake, R.K. Yu, Role of Proteoglycans and Glycosaminoglycans in the Pathogenesis of Alzheimer's Disease and Related Disorders : Amyloidogenesis and Therapeutic Strategies — A Review, (2010).

[22] A.J. Krych, A. Pareek, A.H. King, N.R. Johnson, M.J. Stuart, R.J. Williams, Return to sport after the surgical management of articular cartilage lesions in the knee : a meta ‐ analysis. European Society of Sports Traumatology, Knee Surgery, Arthroscopy (ESSKA) (2016).

[23] M.A. Shamekhi, A. Rabiee, H. Mirzadeh, H. Mahdavi, D. Mohebbi-kalhori, B. Eslaminejad, Fabrication and characterization of hydrothermal cross-linked chitosan porous scaffolds for cartilage tissue engineering applications. Mater. Sci. Eng. C. (2017).

[24] L. Kock, C.C. Van Donkelaar, K. Ito, Tissue engineering of functional articular cartilage : the current status, (2012).

[25] B. Poulet, Models to define the stages of articular cartilage degradation in osteoarthritis development, (2017).

[26] B. Fautrel, Economic impact of lower-limb osteoarthritis worldwide: A systematic review of cost-of-illness studies. Osteoarthr. Cartil. (2016).

[27] C.B. Westin, R.B. Trinca, C. Zuliani, I.B. Coimbra, Â.M. Moraes, Differentiation of dental pulp stem cells into chondrocytes upon culture on porous chitosan-xanthan scaffolds in the presence of kartogenin, vol. 80 (2017).

[28] L. Moroni, D. Seliktar, J. Elisseeff, Biomimetics of the Extracellular Matrix: An Integrated Three- Dimensional Fiber-Hydrogel Composite for Cartilage Tissue Engineering, vol. 7 (2012).

[29] L. Ning, X. Chen, A brief review of extrusion-based tissue scaffold bio-printing, (2017).

[30] V. Rai, M.F. Dilisio, N.E. Dietz, D.K. Agrawal, Review Article Recent strategies in cartilage repair : A systemic review of the scaffold development and tissue engineering, (2017).

[31] X. Wang, B. Ding, B. Li, Biomimetic electrospun nanofibrous structures for tissue engineering. Mater. Today. vol. 16 (2013).

[32] J.W. Gunn, S.D. Turner, B.K. Mann, Adhesive and mechanical properties of hydrogels influence neurite extension, (2004).

[33] P.A. Wieringa, M. Ahmed, T. André, F. Damanik, B.Q. Le, A combinatorial approach towards the design of nanofibrous scaffolds for chondrogenesis OPEN A combinatorial approach towards the design of nanofibrous scaffolds for chondrogenesis. Nat. Publ. Gr. (2015).

[34] L. Vikingsson, J.A. Gómez-tejedor, G.G. Ferrer, J.L.G. Ribelles, An experimental fatigue study of a porous scaffold for the regeneration of articular cartilage. J. Biomech. 48 (2015).

[35] S. Hsu, S. Chang, H. Yen, S.W. Whu, C. Tsai, D.C. Chen, Evaluation of Biodegradable Polyesters Modified by Type II Collagen and Arg-Gly-Asp as Tissue Engineering Scaffolding Materials for Cartilage Regeneration, vol. 30 (2006).

[36] I.E. Palam, V. Arcadio, S.D. Amone, M. Biasiucci, G. Gigli, B. Cortese, Therapeutic PCL scaffold for reparation of resected osteosarcoma defect, (2017).

[37] L. Vikingsson, G.G. Ferrer, J.A. Go, J.L. Go, An “ in vitro ” experimental model to predict the mechanical behavior of macroporous scaffolds implanted in articular

cartilage, vol. 32 (2014).

[38] B. Khozoee, R. Mafi, P. Mafi, W. Khan, Mechanical stimulation of human derived cells in bioreactors for articular cartilage tissue engineering – a systematic review of the literature with a focus on stimulation protocols, (n.d.).

[39] L.M. Kock, A. Ravetto, C.C. Van Donkelaar, J. Foolen, P.J. Emans, K. Ito, Tuning the differentiation of periosteum-derived cartilage using biochemical and mechanical stimulations. Osteoarthr. Cartil. vol. 18 (2010).

[40] J.C.H. Leijten, F.D. Deus, I.B.F. Costa, A Dual Flow Bioreactor with Controlled Mechanical, vol. 19 (2013).

[41] Y. Jung, S. Kim, Y.H. Kim, S.H. Kim, The effects of dynamic and three-dimensional environments on chondrogenic differentiation of bone marrow stromal cells, (2009).

[42] S. Zhong, D. Ph, Y. Zhang, D. Ph, C.T. Lim, D. Ph, Fabrication of Large Pores in Electrospun Nanofibrous Scaffolds for Cellular Infiltration : A Review, vol. 18 (2012).

[43] Y. Yang, I. Wimpenny, M. Ahearne, Portable nanofiber meshes dictate cell orientation throughout three-dimensional hydrogels, Nanomedicine Nanotechnology. Biol. Med. vol. 7 (2011).

[44] Z. Heydari, D. Mohebbi-kalhori, M.S. Afarani, Engineered electrospun polycaprolactone (PCL)/octacalcium phosphate (OCP) scaffold for bone tissue engineering. Mater. Sci. Eng. C. (2017).

[45] S. Ramazani, M. Karimi, Aligned poly (ε -caprolactone)/ graphene oxide and reduced graphene oxide nanocomposite nanofibers : Morphological , mechanical and structural properties. Mater. Sci. Eng. C. vol. 56 (2015).

[46] J. Zhang, H. Liu, H. Xu, J. Ding, X. Zhuang, X. Chen, F. Chang, J. Xu, Z. Li, Molecular weight-modulated electrospun poly(epsilon-caprolactone) membranes for postoperative adhesion prevention. RSC Adv. 4 (2014).

[47] C.J. Luo, E. Stride, M. Edirisinghe, Mapping the Influence of Solubility and Dielectric Constant on Electrospinning Polycaprolactone Solutions, (2012).

[48] J. Dias, P. Bártolo, Morphological characteristics of electrospun PCL meshes – the influence of solvent type and concentration. Elsevier. vol. 5 (2013).

[49] A. Cipitria, A. Skelton, T. R. Dargaville, P. D. Dalton and D. W. Hutmacher, Design, fabrication and characterization of PCL electrospun scaffolds—a review, (2011).

[50] J. Song, H. Gao, G. Zhu, X. Cao, X. Shi, Y. Wang, The preparation and characterization of polycaprolactone / graphene oxide biocomposite nano fi ber

scaffolds and their application for directing cell behaviors. Carbon N. Y. vol. 95 (2015).

[51] R. Scaffaro, F. Lopresti, A. Maio, L. Botta, S. Rigogliuso, G. Ghersi, Electrospun PCL / GO-g-PEG structures : Processing-morphology- properties relationships, Compos. Part A. vol. 92 (2017).

[52] Y. Zhang, H. Ouyang, C.T. Lim, S. Ramakrishna, Z. Huang, Electrospinning of Gelatin Fibers and Gelatin / PCL Composite Fibrous Scaffolds, (2004).

[53] D. Kołbuk, P. Sajkiewicz, K. Maniura-weber, G. Fortunato, Structure and morphology of electrospun polycaprolactone / gelatine nanofibres, vol. 49 (2013).

[54] E. Kostakova, M. Seps, P. Pokorny, D. Lukas, Study of polycaprolactone wet electrospinning process, vol. 8 (2014).

[55] J.A.M. Steele, S.D. Mccullen, A. Callanan, H. Autefage, M.A. Accardi, D. Dini, M.M. Stevens, Combinatorial scaffold morphologies for zonal articular cartilage. Acta Biomater. vol. 10 (2014).

[56] G. Yang, H. Lin, B.B. Rothrauff, S. Yu, R.S. Tuan, Multilayered polycaprolactone / gelatin fiber-hydrogel composite for tendon tissue engineering. ACTA Biomater. (2016).

[57] W. Li, K.G. Danielson, P.G. Alexander, R.S. Tuan, Biological response of chondrocytes cultured in three- dimensional nanofibrous poly (♪ -caprolactone) scaffolds, (2003).

[58] S. Wong, A. Baji, S. Leng, Effect of fiber diameter on tensile properties of electrospun poly(epsilon-caprolactone), vol. 49 (2008).

[59] W. Li, H. Chiang, T. Kuo, H. Lee, C. Jiang, R.S. Tuan, Evaluation of articular cartilage repair using biodegradable nanofibrous scaffolds in a swine model : a pilot study, (2009).

[60] L.A. Bosworth, L. Turner, S.H. Cartmell, State of the art composites comprising electrospun fibres coupled with hydrogels : a review, Nanomedicine Nanotechnology. Biol. Med. vol. 9 (2013).

[61] M.L.A. Silva, A. Martins, P. Costa, S. Faria, M. Gomes, R.L. Reis, N.M. Neves, Cartilage Tissue Engineering Using Electrospun PCL Nanofiber Meshes and MSCs, (2010).

[62] F. Ghorbani, L. Moradi, S. Bonakdar, A. Droodinia, F. Safshekan, M.B. Shadmehr,

In-vivo characterization of a 3D hybrid scaffold based on PCL/ decellularized aorta for tracheal tissue engineering. Mater. Sci. Eng. C. (2017).

[63] R. Augustine, S. K. Nethi, N. Kalarikkal, S. Thomas, C. R. Patra, Electrospun polycaprolactone (PCL) scaffolds embedded with europium hydroxide nanorods (EHNs) with enhanced vascularization and cell proliferation for tissue engineering applications. J. Mater. Chem. B. (2017).

[64] C. Ko, K. Ku, S. Yang, T. Lin, S. Peng, Y. Peng, In vitro and in vivo co-culture of chondrocytes and bone marrow stem cells in photocrosslinked PCL – PEG – PCL hydrogels enhances cartilage formation, (2013).

[65] N. Fu, J. Liao, S. Lin, K. Sun, T. Tian, B. Zhu, Y. Lin, PCL film promotes cartilage regeneration in vivo, (2016).

[66] B. Chaudhuri, B. Mondal, S. Kumar, S.C. Sarkar, Myoblast differentiation and protein expression in electrospun graphene oxide (GO) -poly (ε -caprolactone , PCL) composite meshes. Mater. Lett. vol. 182 (2016).

[67] A. F. Girão, G. Gonçalves, K.S. Bhangra, G. James B. Phillips, J. Knowles, Hurietta, M.K. Singh, I. Bdkin, A. Completo, and P.A.A.P. Marques, Electrostatic self-assembled graphene oxide-collagen scaffolds towards a three-dimensional microenvironment for biomimetic applications. RSC Adv. (2016).

[68] M.V. Robi Kelc, Jakob Naranda, Kuhta Matevz, The Physiology of Sports Injuries and Repair Processes, (2014).

[69] W.D. Callister, Materials Science and Engineering, n.d.

[70] Y.S. Wenxu Li, Duo Wang, Wen Yang, Compressive mechanical properties and microstructure of PVA-HA hydrogels for cartilage repair. RSC Adv. Pap. (2016).

[71] A. Completo, C. Bandeiras, F. Fonseca, Comparative assessment of intrinsic mechanical stimuli on knee cartilage and compressed agarose constructs, vol. 44 (2017).

[72] F. Liu, M. Kozanek, A. Hosseini, S.K. Van De Velde, T.J. Gill, H.E. Rubash, G. Li, In vivo tibiofemoral cartilage deformation during the stance phase of gait. J. Biomech. vol. 43 (2010).

[73] M.S. Kim, G.H. Kim, Highlyporouselectrospun3Dpolycaprolactone/β-TCPbiocomposites for tissueregeneration. Mater. Lett. 120 (2014).

[74] E.P. N. Bölgen, Y.Z.Menceloglu, K. Acatay, I. Vargel, In vitro and in vivo degradation of non-woven materials made of poly (ε -caprolactone) nanofibers

prepared by electrospinning under different conditions, vol. 16 (2005).

[75] F. Croisier, A. Duwez, C. Jérôme, A.F. Léonard, K.O. Van Der Werf, P.J. Dijkstra, M.L. Bennink, Mechanical testing of electrospun PCL fibers. Acta Biomater. vol. 8 (2012).

[76] V. Thomas, M. V Jose, S. Chowdhury, J.F. Sullivan, R. Dean, Y.K. Vohra, Mechano-morphological studies of aligned nanofibrous scaffolds of polycaprolactone fabricated by electrospinning, (2012).

[77] D.E.T. Shepherd, B.B. Seedhom, The " instantaneous " compressive modulus of human articular cartilage in joints of the lower limb, (1999).

[78] H. Kwon, N.K. Paschos, J.C. Hu, K. Athanasiou, Articular cartilage tissue engineering : the role of signaling molecules. Cell. Mol. Life Sci. (2016).

[79] Z. Izadifar, X. Chen, W. Kulyk, Strategic Design and Fabrication of Engineered Scaffolds for Articular Cartilage Repair. J. Funct. Biomater. (2012).

[80] R. Liu, T. Gong, K. Zhang, C. Lee, Graphene oxide papers with high water adsorption capacity for air dehumidification. Sci. Rep. (2017).

[81] A.L. Sisson, D. Ekinci, A. Lendlein, The contemporary role of ε -caprolactone chemistry to create advanced polymer architectures. Polymer, (2013).

[82] C. Yu, B. He, M. Xiong, H. Zhang, L. Yuan, L. Ma, W. Dai, J. Wang, X. Wang, X. Wang, Q. Zhang, Biomaterials The effect of hydrophilic and hydrophobic structure of amphiphilic polymeric micelles on their transport in epithelial MDCK cells. Biomaterials. vol. 34 (2013).

[83] D.D.D. Dominik R. Haudenschild, Jianfen Chen, Nikolai Steklov, Martin K. Lotz, Characterization of the Chondrocyte Actin Cytoskeleton in Living Three-Dimensional Culture: Response to Anabolic and Catabolic Stimuli, vol. 6 (2010).

[84] S.A. Mahmod, S. Snigh, I. Djordjevic, Y. Mei, Phytoestrogen (Daidzein) Promotes Chondrogenic Phenotype of Human Chondrocytes in 2D and 3D Culture Systems. Tissue Eng. Regen. Med. (2017).

[85] M.M.J. Caron, P.J. Emans, M.M.E. Coolsen, L. Voss, D.A.M. Surtel, A. Cremers, L.W. Van Rhijn, T.J.M. Welting, Redifferentiation of dedifferentiated human articular chondrocytes : comparison of 2D and 3D cultures. Osteoarthr. Cartil. 20 (2012).

[86] C. Biosensors, R. Edmondson, J.J. Broglie, A.F. Adcock, L. Yang, Three-Dimensional Cell Culture Systems and Their Applications in Drug Discovery and Cell-Based Biosensors, vol. 12 (2014).

[87] K. A. Athanasiou, E. M. Darling, J. C. Hu, G. D. DuRaine, A. H. Reddi, Articular Cartilage. CRC Press. (2017).

[88] P. G. Bush and A. C. Hall, The volume and morphology of chondrocytes within non-degenerate and degenerate human articular cartilage. OsteoArthritis and Cartilage (2003).

[89] R.A. Stockwell, Biology of Cartilage Cells. Cambridge University Press (1979).

[90] R.A.Freitas Jr., Nanomedicine, Volume I: Basic Capabilities. LANDES BIOSCIENCE (1999).

[91] L. Qi, E.K. Knapton, X. Zh, T. Zhang, C. Gu, Y. Zhao, Pre-culture Sudan Black B treatment suppresses autofluorescence signals emitted from polymer tissue scaffolds. Sci. Rep. (2017).

[92] H. R. Thomas, C. Vallés, R. J. Young, I. A. Kinloch, N. R. Wilson and J. P. Rourke, Identifying the fluorescence of graphene oxide. Journal of Materials Chemistry C (2013).

[93] J. Shang, J. Li, W. Ai, T. Yu, G.G. Gurzadyan, The Origin of Fluorescence from Graphene Oxide, (2012).

[94] J.O. Brien, I. Wilson, T. Orton, Ë. Pognan, Investigation of the Alamar Blue (resazurin) fluorescent dye for the assessment of mammalian cell cytotoxicity, (2000).

[95] B. Page, M. Page, C. Noël, A new fluorometric assay for cytotoxicity measurements in vitro, (1993).

[96] C.Divieto *et al.*l, Uncertainty analysis of cell counting by metabolic assays. Journal Physics: Conference Series (2013).

[97] K. Wang, J. Ruan, H. Song, J. Zhang, Y. Wo, S. Guo, D. Cui, Biocompatibility of Graphene Oxide, (2011).

[98] K. Liao, Y. Lin, C.W. Macosko, C.L. Haynes, Cytotoxicity of Graphene Oxide and Graphene in Human Erythrocytes and Skin Fibroblasts, (2011).

[99] S. Das, S. Singh, V. Singh, D. Joung, J.M. Dowding, J. Anderson, L. Zhai, S.I. Khondaker, W.T. Self, S. Seal, Oxygenated Functional Group Density on Graphene Oxide : Its Effect on Cell Toxicity, (2013).

[100] H. Kweon, M. Kyong, I. Kyu, T. Hee, H. Chul, H. Lee, J. Oh, T. Akaike, C. Cho, A novel degradable polycaprolactone networks for tissue engineering, vol. 24 (2003).

[101] P. Torricelli, M. Gioffrè, A. Fiorani, S. Panzavolta, C. Gualandi, M. Fini, M. Letizia, A. Bigi, Co-electrospun gelatin-poly (L -lactic acid) scaffolds : Modulation of mechanical properties and chondrocyte response as a function of composition. Mater. Sci. Eng. C., vol. 36 (2014).

ANNEXS

The quality and innovation of the scientific work reported in this thesis was already been recognized by the scientific community, as proof the recent acceptances for oral and poster presentation in both national and international congresses:

Annex 1: Poster titled “An adaptive biomimetic graphene-oxide-collagen scaffold for tissue engineering applications” presented at the GRAPHENE FLAGSHIP Conference, September 2017, Athens, Greece.

List of authors: André F. Girão, Gonçalo Ramalho, António Completo and Paula A. A. P. Marques

Annex 2: Submitted abstract titled “Design and fabrication of biomimetic 3D anisotropic fibrous scaffolds for cartilage tissue engineering applications” at the 15th International Symposium on Computer Methods in Biomechanics and Biomedical Engineering and 3rd Conference on Imaging and Visualization, March 2018, Lisbon, Portugal.

List of authors: André F. Girão, Ângela Semitela, Gonçalo Ramalho, Paula A.A.P. Marques and António Completo

Annex 3: Submitted abstract titled “Cellular response to anisotropic fibrous/porous electrospun scaffolds for cartilage tissue engineering” at the 15th International Symposium on Computer Methods in Biomechanics and Biomedical Engineering and 3rd Conference on Imaging and Visualization, March 2018, Lisbon, Portugal.

List of authors: Ângela Semitela, André F. Girão, Gonçalo Ramalho, António Completo and Paula A.A.P. Marques.

5.2. Annex I

An adaptive biomimetic graphene-oxide-collagen scaffold for tissue engineering applications

André F. Girão [1], Gonçalo Ramalho [1], António Completo [1], Paula A.A.P. Marques [1]

[1] *TEMA, Department of Mechanical Engineering, University of Aveiro, Portugal*

During the last few years, graphene has being playing a central role in a wide range of biomedical engineering strategies, including biosensors, brain-computer-interactions and regenerative medicine. In fact, and regarding this last topic, graphene based materials are being increasingly used in tissue engineering (TE) applications due to their capability of combining their excellent electrical and mechanical features with the properties of biomaterials such as polymers with the final purpose of recreating *in vitro* complex 3D extracellular matrix architectures able to support an enhanced cellular response [1].

Thus, in this work, we successfully explored the potential of the graphene oxide (GO) sheets to act as functional building blocks by using collagen as physical crosslinker. Indeed, the electrostatic interactions between the two materials have allowed the fabrication of a self-assembled hydrogel capable of providing a suitable porous network for both static and dynamic cell culture protocols [2]. Additionally, and complementary to its enhanced chemical, mechanical and morphological properties, the GO-collagen scaffold also revealed an impressive versatility since its bulk characteristics can be easily modified to match specific TE aims. Indeed, by either adapting its conductivity via a reduction process or modulating its topographic cues via the incorporation of a 3D anisotropic Polycaprolactone (PCL) electrospun network, the GO-collagen scaffold proved to be able to mimic different cellular microenvironments such as neural and cartilage, respectively.

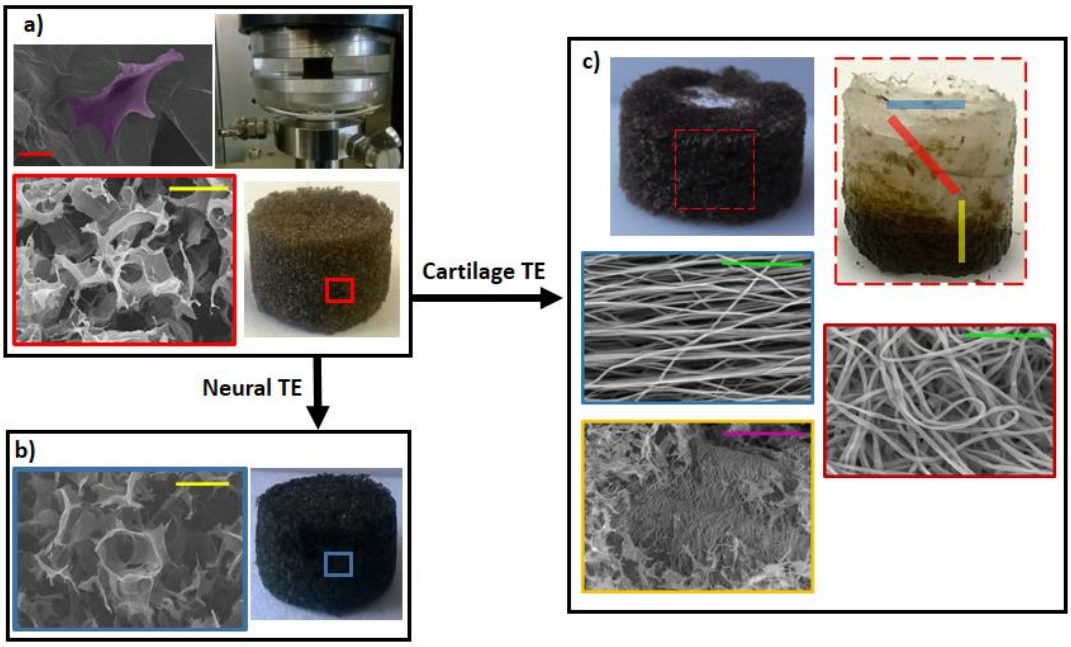

Fig. 1. GO-collagen scaffold as a versatile biomimetic microenvironment. a) GO-collagen scaffold porous network biocompatibility and dynamic stimulation assays; b) GO-collagen scaffold after a reduction process for neural TE applications; c) PCL-GO-collagen porous-fibrous scaffold for cartilage TE applications. Scale bars: red = 20 μm; yellow = 150 μm; green = 50 μm; purple = 500 μm.

References

[1] Goenka, S. et al., J Control Release, 10, 2014

[2] Girão et al., RSC Adv., 6, 2016

Acknowledgements: FCT with the projects: IF/00917/2013/CP1162/CT0016; PTDC/EMS-TEC/3263/2014 and Programa Operacional Competitividade e Internacionalização through the project POCI-01-0145-FEDER-016574.

5.3. Annex II

Design and fabrication of biomimetic 3D anisotropic fibrous scaffolds for cartilage tissue engineering applications

André F. Girão, Ângela Semitela, Gonçalo Ramalho, Paula A.A.P. Marques and António Completo

The major challenge and also the main opportunity of cartilage tissue engineering is to recreate *in vitro* the depth dependent nanostructural organization of the fibrous collagen network that comprises the native cartilaginous tissue. In fact, the fibre size and orientation rearrangement of the cartilage natural extracellular matrix progresses from perpendicular to the subchondral bone surface in the deepest zone, to random in the middle zone and to parallel in the superficial region, leading to anatomically and functionally complementary features that are responsible for the biochemical and mechanical properties of this tissue. Though the encouraging results of both fibrous and porous scaffolds during the past few years, none of the followed methodologies is currently capable of guaranteeing an optimal balance between biological features, mechanical properties and suitable topographic cues.

Thus, in this study, with the purpose of accurately recreating each cartilaginous zone, we purpose a versatile design and fabrication strategy involving the combination of different electrospinning set ups that are sequentially used to control the size and alignment of the Polycaprolactone (PCL) fibres towards a 3D structure. In this way, we were able to adapt the methodology in order to develop alternative fibrous scaffolds with distinct anisotropy properties capable of offering singular mechanical and topographic characteristics and therefore theoretically influence cell behaviour differentially. The morphology of the 3D electrospun scaffolds together with their individual fibrous zones were analysed via SEM and their mechanical properties were evaluated via static and dynamic (via a bioreactor) compressive and tensile tests.

The results confirmed that although the mechanical and swelling properties of the electrospun scaffolds are related with the specific anisotropic organization used in each design, all the scaffolds show compatible features for cartilage cell culture protocols and therefore the potential of being used as alternative enhanced cellular microenvironments capable of promoting cartilage regeneration using different pathways.

This work was supported by the funding of Program COMPETE-FEDER, Programa Operacional Competitividade e Internacionalização through the project POCI-01-0145-FEDER-016574 and by Fundação para a Ciencia e Tecologia I.P. (FCT, IP) through the project PTDC/EMS-TEC/3263/2014. The authors thank to FCT for the PhD grants SFRH/BD/130287/2017 and SFRH/BD/133129/2017.

Keywords: cartilage tissue engineering; anisotropic scaffold; electrospinning

5.4. Annex III

Cellular response to anisotropic fibrous/porous electrospun scaffolds for cartilage tissue engineering

Ângela Semitela, André F. Girão, Gonçalo Ramalho, António Completo and Paula A.A.P. Marques

Tissue engineering (TE) strategies for repairing and regenerating articular cartilage face critical challenges to approximate the biochemical and biomechanical microenvironment of native tissues. The major challenge of TE cartilage is to mimic their mechanical properties to the native ones. The importance of the arcade-like collagen structure for the load-bearing properties in native cartilage is well emphasized in literature, but few studies have assessed the importance of collagen fibril depth-orientation on the mechanical properties of engineered-cartilage. To generate spatially-varying properties into TE-cartilage scaffolds, several combined cell-scaffold methods have been reported. Electrospinning allows the formation of arrays of aligned and random polymer-based nanofibers mats that can be assembled to mimic the structure of the native cartilaginous extracellular matrix. Mechanical stimulation can also be performed in order to create an anisotropic distribution of collagen in engineered-cartilage. Thus, a new series of anisotropic fibrous/porous electrospun scaffolds of polycaprolactone/collagen/graphene were developed and their biocompatibility evaluated with and without mechanical stimulation using a bioreactor. First, anisotropic fibrous layers of PCL with depth-dependent variations in the fibrillar size and orientation were electrospun and then assembled and incorporated within a microporous graphene oxide/collagen structure. Several architectures were produced and tested *in vitro*. For this, a cartilage progenitor cell line was used and the cell metabolic activity, morphology and distribution throughout the scaffolds were accessed. The results, both static and dynamic, revealed that the scaffolds could not only allow cells' adhesion, but also cell proliferation. Overall, polycaprolactone/collagen/graphene oxide scaffolds generated a good cellular response and were able to support cell proliferation. The effect of mechanical stimulation under physiological conditions is discussed. This work was supported by the funding of Program COMPETE-FEDER, Programa Operacional Competitividade e Internacionalização through the project POCI-01-0145-FEDER-016574 and by Fundação para a Ciência e Tecnologia I.P. (FCT, IP) through the project PTDC/EMS-TEC/3263/2014. The authors thank to FCT for the PhD grants SFRH/BD/133129/2017 and SFRH/BD/130287/2017.

Keywords: cartilage tissue engineering, electrospun scaffolds, anisotropic, biocompatibility